1 of 3

NWL Report No. 1913

48-P. #1.25

ROTATING FLOWS OVER A ROTATING DISK

by

Ernst W. Schwiderski and Hans J. Lugt
Computation and Analysis Laboratory

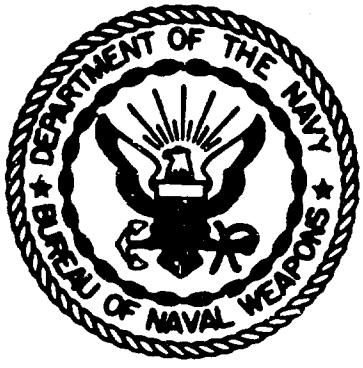

U. S. NAVAL WEAPONS LABORATORY
DAHLGREN, VIRGINIA

U. S. Naval Weapons Laboratory
Dahlgren, Virginia

Rotating Flows Over a Rotating Disk

by

Ernst W. Schwiderski and Hans J. Lugt
Computation and Analysis Laboratory

NWL REPORT NO. 1913

Task Assignment
NO. R360FR103/2101/R01101001

April 1964

TABLE OF CONTENTS

ABSTRACT

Local boundary layer approximations of first order are computed for axisymmetric motions which rotate over a rotating disk in the same and opposite directions. The secondary motions, which are produced by the friction forces at the rotating disk, are essentially of pure stagnation type, distorted stagnation type, cell type, and pure wake type. Critical Reynolds numbers of steady laminar motions which are attached to the disk are computed. They reveal stability properties of rotating flows which are of importance in practical applications.

FOREWORD

This work was sponsored by the Naval Weapons Laboratory Foundational Research Program. It was performed in the Computation and Analysis Laboratory as part of the project Fluid Dynamics with Applications to the Atmosphere and Oceans (R360FR103/2101/R01101001).

The date of completion was 1 April 1964.

Approved for Release:

RALPH A. NIEMANN
Acting Technical Director

1. Introduction

Axisymmetric rotating flows over a rotating disk of infinite dimensions have been studied in [1 through 8]. Recently the special problems of von Kármán and Bödewadt have been reinvestigated in [9 and 12]. Adjusted local boundary layer approximations of first order, which were introduced in [10 and 11], have been obtained for both problems. The heat transfer from a rotating disk into a fluid asymptotically at rest, which is computed in [9], agrees well with empirical results.

In the present paper the local boundary layer approximations of first order derived in [12] are generalized to axisymmetric motions which rotate over a rotating disk of infinite dimensions. Numerical results are computed and discussed for a variety of Reynolds numbers and for cases in which the disk is rotating in the same sense and in the opposite sense as the fluid far away from the disk. In particular, critical Reynolds numbers for steady laminar motions which are attached to the surface of the disk are computed and displayed.

2. Construction of Rotating Flows

A viscous incompressible fluid may be contained in a circular cylinder which is normal to a disk of equal diameter (see Fig. 1). If the cylinder is rotating at a constant angular velocity $\omega_\infty (\geq 0)$, then the fluid far away from the disk will essentially assume the same angular velocity ω_∞. Near the disk the fluid rotates with the angular velocity $\omega_0 (\gtrless 0)$ of the disk. Furthermore, due to the friction forces at the disk, fluid will be ejected or drawn through a slit of

negligible size which may be provided between the cylinder and the disk. Hence, the resulting rotation of the fluid becomes superposed by a secondary flow as sketched in Figs. 1 a. through 1 c..

In order to investigate exclusively the effects of the friction forces at the disk on the rotating fluid, the surface of the cylinder wall may be assumed to glide freely with the generated axial flow. For the sake of simplicity, only the flow model of infinite diameter and height is considered which is dynamically similar to one of the finite models described. As was pointed out in [12] the infinite flow model is specified by the constant kinematic viscosity ν of the fluid, by the two angular velocities ω_0 and ω_∞, and by the characteristic length $\ell (> 0)$ of the motions considered. The latter parameter (see [12]) may be defined as the geometric mean of the axial thickness a and twice the axial radius of curvature 1/b of a properly defined boundary layer along the solid disk (see Eqs. (10) and (12)). Accordingly, a finite flow model and an infinite model are considered geometrically similar if they agree in their characteristic lengths.

For the mathematical description of the flow a coaxial cylindrical coordinate system (r,φ,z) may be introduced so that $z = 0$ designates the solid surface of the disk. If (u,v,w) denotes the corresponding velocity vector, p the variable pressure, and ρ the constant density, then the motion is governed by the Navier-Stokes equations:

$$uu_r + wu_z - \frac{v^2}{r} = -\frac{1}{\rho} p_r + \nu\left[u_{rr} + \left(\frac{u}{r}\right)_r + u_{zz}\right] \qquad (1)$$

$$uv_r + wv_z + \frac{uv}{r} = + \nu\left[v_{rr} + \left(\frac{v}{r}\right)_r + v_{zz}\right] \tag{2}$$

$$uw_r + ww_z = -\frac{1}{\rho} p_z + \nu\left[w_{rr} + \frac{1}{r} w_r + w_{zz}\right] \tag{3}$$

$$(ru)_r + (rw)_z = 0 . \tag{4}$$

In order to introduce dimensionless quantities it is useful to define

$$\Omega = \omega_0 - \omega_\infty \qquad \text{and} \qquad \varkappa = \frac{\omega_\infty}{\Omega} \tag{5}$$

respectively as the "characteristic angular velocity" and the "characteristic velocity ratio" of the motion considered. In contrast to other definitions (see [1, 6, 8]) the expressions (5) appear to be advantageous because they become meaningless ($\Omega = 0$, $\varkappa = \infty$) only for the trivial rotation which is defined by $\omega_0 = \omega_\infty$.

In the dimensionless dependent variables

$$u = \Omega r U, \quad v = \Omega r V, \quad w = w_\infty W, \quad \frac{p}{\rho} = \frac{\Omega^2 r^2}{2} \varkappa^2 - \frac{w_\infty^2}{2} P \tag{6}$$

the solution of the Navier-Stokes equations under consideration is determined by the boundary data (see [12])

$$z = 0, \ |r| < \infty: \quad U = 0, \quad V = 1 + \varkappa, \quad W = 0 , \tag{7}$$

$$\left.\begin{array}{l} z = \infty, \ |r| \leq \infty \\ z > 0, \ |r| = \infty \end{array}\right\}: U = 0, \quad V = \varkappa , \quad W = 1, \tag{8}$$

where w_∞ is a certain constant which must be determined simultaneously with the integral.

Following derivations presented in [12] it is helpful to introduce the limiting line of the boundary layer along the disk

$$z = \delta(r) = a - br^2 + cr^4 + \ldots \quad (r \leq r_0) \tag{9}$$

by the ϵ-condition

$$z = \delta(r): \quad |V - \kappa| = \epsilon \qquad (\epsilon > 0)\ . \tag{10}$$

A local boundary layer approximation of first order, which is adjusted to the curvature of the boundary layer around the axis of rotation r = 0, is of the form

$$U = -\dot{G}(\eta),\ V = V(\eta),\ W = \frac{2\Omega}{w_\infty}\,\ell G(\eta),\ P = \frac{4\Omega^2}{w_\infty^2}\,\ell^2 H(\eta), \tag{11}$$

provided the motion is steady, laminar, and attached to the disk. In these equations the dot denotes the derivative with respect to the single dimensionless variable

$$\eta = \sqrt{ab}\,\frac{z}{\delta(z)} = \frac{z/\ell}{1 - \frac{r}{\ell}^2 + \ldots}\ , \quad \ell = \sqrt{a/b} \tag{12}$$

where ℓ is by definition the characteristic length of the motion. After [12] the first order approximation (11) is the integral of the differential equations

$$\dddot{G} + 8\eta\ddot{G} = -R(\kappa^2 + \dot{G}^2 - 2G\ddot{G} - V^2 - 4\eta\dot{H}) \tag{13}$$

$$\ddot{V} + 8\eta\dot{V} = -2R(\dot{G}V - G\dot{V}) \tag{14}$$

$$\dot{H} = 2G\dot{G} - \frac{1}{R}\,(\ddot{G} + 4\eta\dot{G}) \tag{15}$$

which satisfies the boundary conditions

$$\eta = 0: \quad G = 0,\ \dot{G} = 0,\ V = 1 + \kappa \tag{16}$$

$$\eta = \infty: \quad G = G_\infty,\ V = \kappa,\ H = G_\infty^2\ . \tag{17}$$

The dimensionless parameter

$$R = \frac{\Omega}{\nu}\,\ell^2 \tag{18}$$

can be interpreted as the Reynolds number of the motion. It may be

mentioned that by this definition the Reynolds number assumes positive and negative values according as Ω is positive or negative (see Eq. (5)). This convention appears to be useful since the axial flow is expected to be of stagnation type (directed against the disk) for $\Omega = \omega_0 - \omega_\infty > 0$ (see [13]). For $\Omega = \omega_0 - \omega_\infty < 0$ the axial flow will generally be of wake type (directed away from the disk) with the few exceptions displayed in Figs. 1 a. through 1 d.. It may also be noted that by convention (5) the characteristic velocity ratio $\varkappa$ possesses the same sign as Ω and R. In particular, the flows of von Kármán and Bödewadt, which have been investigated in [9 and 12], are characterized by the parameters ($R > 0$, $\varkappa = 0$) and ($R < 0$, $\varkappa = -1$), respectively.

3. Stability of Rotating Flows

Axisymmetric rotating flows over a rotating disk have been computed for various Reynolds numbers R and velocity ratios $\varkappa$ (Tables 1-12). Selected examples are displayed in Figs. 2 through 14. As in von Kármán's case $\varkappa = 0$ (see [12]) numerical calculations of rotating flows with $\varkappa \geq 0$ (i.e., $\omega_0 > \omega_\infty > 0$) indicated no symptoms of instability for any Reynolds number $R(> 0)$. The secondary flow is of pure stagnation type (see Fig. 1a) and all velocity profiles are free of inflection points which characterize unstable motions.

For velocity ratios $\varkappa < 0$ (i.e., $\omega_0 < \omega_\infty (> 0)$) all rotating flows become unstable beyond a certain "critical Reynolds number" $R_c(\varkappa) (< 0)$ which depends on the value of $\varkappa$. Fig. 2 shows the corresponding critical curve which has been approximately determined at several points. These numerical calculations demonstrated distinctly two different kinds of instabilities below and above $\varkappa \approx -1/2$ (i.e., $\omega_\infty \approx -\omega_0$).

For $\varkappa < -1/2$ (i.e., $\omega_\infty > |\omega_0|$) the instability is of the same sort as in Bödewadt's case $\varkappa = -1$ (see [12]). The secondary flow is of pure wake type (see Fig. 1c.) which begins to oscillate in the upper portion of the boundary layer when the Reynolds number R exceeds its critical value R_c. This experience indicates that the oscillating solutions, which were found in [1, 6, 8] for $\varkappa \leq -1$ (i.e., $\omega_\infty > \omega_0 \geq 0$), should also exist for the $\varkappa$-range $-1/2 \leq \varkappa < -1$. Unfortunately, Rogers and Lance [6] inspected the entire $\varkappa$-range with the exception of this interval. However, as was pointed out in [12 and 13] the nonexistence of a proper solution to the boundary value problem (13) through (17) is an indication that in reality the motion is separated from the surface of the disk (see the tea-cup experiment described in [12]) and violates the hypothesis (11).

For the $\varkappa$-range $-1/2 < \varkappa < 0$ (i.e., $0 < \omega_\infty < -\omega_0$) the instability beyond a critical Reynolds number $R_c(\varkappa)$ arises in the lower portion of the boundary layer through the occurrence of two inflection points in the tangential velocity profile (see [13]). The solutions of the differential equations (13), (14), and (15) appear to be unbounded at infinity and it is impossible to satisfy the boundary conditions (17). In the $\varkappa$-range considered the secondary flows are either of the "cell type" sketched in Figs. 1d. and 1c. or of, the "distorted stagnation type" plotted in Fig. 1b., provided the absolute value of the Reynolds number R is sufficiently large. When the Reynolds number R exceeds the critical value $R_c(\varkappa)$, the whole flow field seems to be affected by the friction forces at the disk. This explains the nonexistence of a proper solution to the problems considered in [1, 6, 8] for

the same $\varkappa$-range $0 < \varkappa \leq -1/2$. Indeed, these problems are specified among the present problems by infinite Reynolds numbers. Since $\varkappa = -1/6$ (i.e., $\omega_0 = -5\omega_\infty (< 0)$) marks roughly the "limiting cell flow" sketched in Fig. 1c. for large Reynolds numbers, the instability will be most severe for the cell-type range $-1/2 \leq \varkappa \leq -1/6$ and less severe for the distorted stagnation-type range $-1/6 < \varkappa < 0$. In fact, this confirms and explains the numerical experience of Rogers and Lance as described in [6].

For practical applications it is important to observe, that according to the curve of critical Reynolds numbers presented in Fig. 2, the instability of rotating motions increases with increasing velocity ratios $(-\varkappa) > 0$, i.e., with decreasing characteristic angular velocity $(-\Omega) = \omega_\infty - \omega_0 > 0$. This significant phenomenon is physically plausible. Indeed, if a fluid rotates at an angular velocity $\omega_\infty (> 0)$ over a disk, the tendency of flow separation will be supported by a slow $(0 < \omega_0 < \omega_\infty)$ rotation of the disk in the same direction. The rotation of the disk in the direction of the rotating fluid acts similarly to an injection of fluid through the disk which decreases the pressure variation along the axis of symmetry (see Fig. 6a.) and, thus, increases the danger of flow separation. On the other side, the tendency of flow separation can be greatly reduced by rotating the disk in opposite direction of the rotating fluid. In this case the rotation of the disk acts like a suction of fluid through the disk which increases the pressure variation along the axis of symmetry (see Fig. 6a.) and, hence, decreases the danger of flow separation.

The phenomenon of flow separation can eventually be eliminated by rotating the disk sufficiently fast in opposite sense of the rotation of the fluid. However, such a rotation produces cell flows or even distorted stagnation flows (see Figs. 1d., 1c., and 1b.) which reach a different kind of critical point. When the Reynolds number approaches its critical value, the friction forces at the surface affect the entire flow field and prevent a proper solution from existing.

4. Flow Patterns of Rotating Motions

In Figs. 3a. through 6b. the velocity profiles V, $G = w_\infty W/2\Omega\ell$, $\dot{G} = -U$ and the pressure P have been plotted for various velocity ratios $\varkappa$, which have been computed at the constant Reynolds number $|R| = 1$. While the tangential velocity profiles V are essentially congruent for all velocity ratios $\varkappa$, the secondary velocity profiles G and $\dot{G}$ display significant changes especially in the most interesting $\varkappa$-range $-1/3 \leq \varkappa \leq 0$. From the secondary velocity profiles G and $\dot{G}$ one arrives easily at the following five essentially different secondary flow patterns.

a. Pure Stagnation Flows: At $|R| = 1$ the secondary flow is of pure stagnation type within the $\varkappa$-range $-.035 \leq \varkappa < +\infty$ (see Fig. 1a.). The pressure displays the same nonmonotonic behavior as in von Kármán's case $\varkappa = 0$ (see [12] and Figs. 6a. and 6b.) which represents the prototype of these motions. It may be mentioned that the lower limit $\varkappa = -.035$, which has been approximately determined, increases to $\varkappa = 0$ ($\omega_0 > \omega_\infty > 0$) when the Reynolds number $|R|$ increases to infinity.

b. Distorted Stagnation Flows: For the $\varkappa$-range $-.2056 < \varkappa < -.035$ and $R = -1$ the secondary flows are of the distorted stagnation type

sketched in Fig. 1b. In this $\varkappa$-range the pressure is subjected to its greatest change (see Fig. 6b.). When $\varkappa$ varies from the upper limit ($\varkappa = -.035$) to the lower limit ($\varkappa = -.2056$) the pressure changes rapidly from the stagnation type to the wake type and maintains that feature for all lower values of $\varkappa$. In Figs. 7. through 10. a cross-section of distorted stagnation flows is shown for various Reynolds numbers R at the fixed velocity ratio $\varkappa = -.1$. One can see that for the velocity ratio $\varkappa = -.1$ the stagnation character of the secondary flow remains unchanged for all noncritical Reynolds numbers. In fact, the computations indicated that the $\varkappa$-range of distorted stagnation flows changes to approximately the interval $-1/6 < \varkappa < 0$ $(0 < 5\omega_\infty < -\omega_0)$ if the Reynolds numbers R approach their critical values $R_c(\varkappa)$.

c. Limiting Cell Flows: For $R = -1$ and $\varkappa \approx -.2056$ the secondary motion, which is always generated by the rotating fluid at large distances from the disk, vanishes completely and a simple cell flow develops as sketched in Fig. 1c. The pressure assumes essentially the nonmonotonic features of wake flows which were pointed out for Bödewadt flows ($\varkappa = -1$) in [12]. When the Reynolds number $|R|$ increases, the velocity ratio $\varkappa$ of limiting cell flows approaches the value $\varkappa \approx -1/6$ $(5\omega_\infty \approx -\omega_0)$.

d. Cell Flows: Within the $\varkappa$-range $-.3271 < \varkappa < -.2056$ the friction forces at the rotating disk are still strong enough to produce a kind of degenerated stagnation flow near the disk. However, far away from the disk the rotation of the fluid dominates over the effects of the rotation of the disk and produces a wake flow so that a cell flow

develops as sketched in Fig. 1d. Hence, while the pressure undergoes its greatest change in the $\varkappa$-range of distorted stagnation flows, the secondary motion suffers its greatest change in the $\varkappa$-range of cell flows. The graphs in Figs. 11. through 14. display a cross-section of cell flows for various Reynolds numbers R at the fixed velocity ratio $\varkappa = -.22$. As these graphs show the cell type remains unchanged for all noncritical Reynolds numbers provided $\varkappa = -.22$. Computations indicated that the $\varkappa$-range of cell flows increases to approximately the interval $-1/2 < \varkappa < -1/6$ $(0 <- \omega_0/5 < \omega_\infty < -\omega_0)$ when the Reynolds number increases in its absolute value $|R|$.

e. Pure Wake Flows: In the $\varkappa$-range $-\infty < \varkappa < -.3271$ at $\bar{R} = -1$ the rotation of the fluid far away from the disk determines the entire secondary flow. A pure wake flow develops as sketched in Fig. 1c. The prototype of these secondary flows is the wake flow which was described in [12] in Bödewadt's case $\varkappa = -1$. When the Reynolds number $|R|$ increases toward its critical value $R_c(\varkappa)$, the $\varkappa$-range of pure wake flows seems to approach the semi-infinite interval $-\infty < \varkappa < -1/2$ $(\omega_\infty > |\omega_0|)$.

REFERENCES

[1] BATCHELOR, G. H., Note on a class of solutions of the Navier-Stokes equations representing steady rotationally symmetric flow, Quarterly Journal of Mechanics and Applied Mathematics, 4, (1951), 29-41.

[2] BÖDEWADT, U. T., Die Drehströmung über festem Grunde, ZAMM, 20, (1940), 241-253.

[3] VON KÁRMÁN, Über laminare und turbulente Reibung, ZAMM, 1, (1921),244-247.

[4] MACK, L. M., The laminar boundary layer on a disk of finite radius in a rotating flow, Jet Propulsion Laboratory, Techn. Rep. No. 32-224, May 20, 1962.

[5] MOORE, F. K., Three-dimensional boundary layer theory, Advances in Applied Mechanics, IV, (1956), 159-228.

[6] ROGERS, M. H. and LANCE, G. N., The rotationally symmetric flow of a viscous fluid in the presence of an infinite rotating disk, Journal of Fluid Mechanics, 7, (1960), 617-631.

[7] SCHLICHTING, H., Boundary Layer Theory, Fourth Edition, 1960.

[8] STEWARTSON, K., On the Flow between Two Rotating Coaxial Disks, Proc. Cambridge Phil. Soc., 49, (1953), 333-341.

[9] LUGT, H. J. and SCHWIDERSKI, E. W., Temperature Distribution in Rotating Flows Normal to a Flat Surface. To be published.

[10] SCHWIDERSKI, E. W. and LUGT, H. J., On the Axisymmetric Vortex Flow Over a Flat Surface. To be published.

[11] SCHWIDERSKI, E. W. and LUGT, H. J., Vortex Flows Normal to a Flat Surface, Tellus, 15, (1963), No. 3.

[12] SCHWIDERSKI, E. W. and LUGT, H. J., Rotating Flows of von Kármán and Bödewadt, The Physics of Fluids, 7, (1964), No. 6.

[13] SCHWIDERSKI, E. W. and LUGT, H. J., Plane and Axisymmetric Flows Normal to a Flat Plate. To be published.

APPENDIX A

TABLE 1: TANGENTIAL VELOCITY V(|R| = 1)

R	+ 1	+ 1	- 1	- 1	- 1	- 1	- 1	- 1	- 1	- 1	- 1
η \ κ	+ 10	+ 1	-.01	-.035	-.17	-.2056	-.3271	- 1/3	- 2/3	- 2	- 3
.00	.1100+2	.2000+1	.9900	.9650	.8300	.7944	.6729	.6666	.3333	-.1000+1	-.2000+1
.05	.1082+2	.1885+1	.8773	.8523	.7174	.6819	.5604	.5542	.2209	-.1114+1	-.2118+1
.10	.1066+2	.1772+1	.7669	.7419	.6071	.5716	.4502	.4440	.1107	-.1226+1	-.2234+1
.15	.1051+2	.1665+1	.6608	.6359	.5012	.4657	.3443	.3381	.4825-2	-.1334+1	-.2344+1
.20	.1039+2	.1564+1	.5610	.5360	.4014	.3659	.2446	.2383	-.9492-1	-.1435+1	-.2448+1
.25	.1028+2	.1471+1	.4688	.4439	.3093	.2738	.1525	.1463	-.1870	-.1528+1	-.2542+1
.30	.1020+2	.1388+1	.3854	.3605	.2259	.1904	.6917-1	.6295-1	-.2703	-.1612+1	-.2626+1
.35	.1014+2	.1314+1	.3115	.2866	.1520	.1165	-.4771-2	-.1099-1	-.3443	-.1685+1	-.2699+1
.40	.1009+2	.1250+1	.2473	.2224	.8776-1	.5223-1	-.6907-1	-.7530-1	-.4086	-.1749+1	-.2762+1
.45	.1006+2	.1196+1	.1925	.1676	.3296-1	-.2564-2	-.1238	-.1301	-.4634	-.1803+1	-.2815+1
.50	.1003+2	.1151+1	.1468	.1219	-.1280-1	-.4834-1	-.1697	-.1759	-.5092	-.1848+1	-.2858+1
.55	.1002+2	.1115+1	.1094	.8447-1	-.5029-1	-.8584-1	-.2072	-.2134	-.5468	-.1885+1	-.2893+1
.60	.1001+2	.1085+1	.7937-1	.5442-1	-.8038-1	-.1159	-.2373	-.2435	-.5769	-.1914+1	-.2921+1
.65	.1000+2	.1062+1	.5574-1	.3077-1	-.1041	-.1396	-.2610	-.2672	-.6006	-.1937+1	-.2942+1
.70	.1000+2	.1045+1	.3752-1	.1254-1	-.1223	-.1579	-.2793	-.2855	-.6189	-.1954+1	-.2959+1
.75	.1000+2	.1032+1	.2374-1	-.1232-2	-.1361	-.1717	-.2931	-.2994	-.6327	-.1968+1	-.2971+1
.80	.9999+1	.1022+1	.1354-1	-.1144-1	-.1463	-.1819	-.3034	-.3096	-.6429	-.1977+1	-.2980+1
.85	.9999+1	.1015+1	.6128-2	-.1886-1	-.1538	-.1893	-.3108	-.3171	-.6504	-.1984+1	-.2986+1
.90	.9999+1	.1010+1	.8511-3	-.2414-1	-.1591	-.1946	-.3161	-.3224	-.6557	-.1989+1	-.2990+1
.95	.9999+1	.1006+1	-.2831-2	-.2782-1	-.1628	-.1983	-.3198	-.3261	-.6594	-.1993+1	-.2994+1
1.00	.9999+1	.1004+1	-.5350-2	-.3034-1	-.1653	-.2009	-.3224	-.3286	-.6619	-.1995+1	-.2996+1
1.10	.9999+1	.1001+1	-.8149-2	-.3314-1	-.1681	-.2037	-.3252	-.3314	-.6647	-.1998+1	-.2998+1
1.20	.9999+1	.1000+1	-.9316-2	-.3431-1	-.1693	-.2049	-.3264	-.3326	-.6659	-.1999+1	-.2999+1
1.30	.1000+2	.1000+1	-.9765-2	-.3476-1	-.1697	-.2053	-.3268	-.3330	-.6664	-.1999+1	-.2999+1
1.40	.1000+2	.1000+1	-.9925-2	-.3492-1	-.1699	-.2055	-.3270	-.3332	-.6665	-.1999+1	-.2999+1

TABLE 2: AXIAL VELOCITY $G = w_\infty W/2\Omega\ell$ ($|R| = 1$)

R	+ 1	+ 1	- 1	- 1	- 1	- 1	- 1	- 1	- 1	- 1	- 1
η \ $\varkappa$	+ 10	+ 1	-.01	-.035	-.17	-.2056	-.3271	- 1/3	- 2/3	- 2	- 3
.00	0	0	0	0	0	0	0	0	0	0	0
.05	-.3180-2	-.5686-3	.1328-3	.1218-3	.6263-4	.4700-4	-.6424-5	-.9166-5	-.1559-3	-.7348-3	-.1145-2
.10	-.1113-1	-.2038-2	.4598-3	.4201-3	.2052-3	.1484-3	-.4532-4	-.5527-4	-.5876-3	-.2685-2	-.4167-2
.15	-.2176-1	-.4085-2	.8901-3	.8096-3	.3742-3	.2592-3	-.1335-3	-.1537-3	-.1232-2	-.5480-2	-.8465-2
.20	-.3342-1	-.6431-2	.1354-2	.1226-2	.5340-3	.3511-3	-.2739-3	-.3060-3	-.2023-2	-.8774-2	-.1349-1
.25	-.4491-1	-.8856-2	.1806-2	.1628-2	.6647-3	.4103-3	-.4589-3	-.5035-3	-.2891-2	-.1226-1	-.1879-1
.30	-.5541-1	-.1119-1	.2213-2	.1986-2	.7582-3	.4337-3	-.6749-3	-.7318-3	-.3778-2	-.1572-1	-.2400-1
.35	-.6450-1	-.1333-1	.2562-2	.2289-2	.8147-3	.4252-3	-.9059-3	-.9742-3	-.4631-2	-.1896-1	-.2885-1
.40	-.7199-1	-.1520-1	.2846-2	.2533-2	.8399-3	.3924-3	-.1136-2	-.1215-2	-.5416-2	-.2186-1	-.3316-1
.45	-.7793-1	-.1678-1	.3070-2	.2722-2	.8413-3	.3443-3	-.1354-2	-.1441-2	-.6109-2	-.2436-1	-.3686-1
.50	-.8245-1	-.1807-1	.3239-2	.2863-2	.8270-3	.2889-3	-.1549-2	-.1644-2	-.6697-2	-.2643-1	-.3991-1
.55	-.8578-1	-.1909-1	.3364-2	.2965-2	.8041-3	.2331-3	-.1718-2	-.1818-2	-.7180-2	-.2811-1	-.4236-1
.60	-.8815-1	-.1987-1	.3452-2	.3035-2	.7780-3	.1814-3	-.1857-2	-.1962-2	-.7564-2	-.2942-1	-.4426-1
.65	-.8978-1	-.2046-1	.3513-2	.3083-2	.7524-3	.1365-3	-.1968-2	-.2076-2	-.7861-2	-.3042-1	-.4570-1
.70	-.9087-1	-.2088-1	.3555-2	.3114-2	.7297-3	.9961-4	-.2054-2	-.2164-2	-.8083-2	-.3115-1	-.4676-1
.75	-.9157-1	-.2118-1	.3581-2	.3134-2	.7108-3	.7052-4	-.2118-2	-.2230-2	-.8245-2	-.3168-1	-.4751-1
.80	-.9201-1	-.2139-1	.3598-2	.3146-2	.6960-3	.4853-4	-.2164-2	-.2278-2	-.8360-2	-.3205-1	-.4804-1
.85	-.9228-1	-.2153-1	.3609-2	.3153-2	.6848-3	.3249-4	-.2197-2	-.2311-2	-.8439-2	-.3230-1	-.4840-1
.90	-.9243-1	-.2163-1	.3615-2	.3157-2	.6767-3	.2119-4	-.2219-2	-.2334-2	-.8492-2	-.3247-1	-.4863-1
.95	-.9252-1	-.2168-1	.3619-2	.3159-2	.6711-3	.1346-4	-.2234-2	-.2349-2	-.8527-2	-.3258-1	-.4879-1
1.00	-.9257-1	-.2172-1	.3621-2	.3160-2	.6673-3	.8341-5	-.2243-2	-.2359-2	-.8550-2	-.3265-1	-.4888-1
1.10	-.9261-1	-.2176-1	.3623-2	.3161-2	.6632-3	.2962-5	-.2253-2	-.2369-2	-.8572-2	-.3272-1	-.4898-1
1.20	-.9262-1	-.2177-1	.3624-2	.3162-2	.6617-3	.9349-6	-.2257-2	-.2373-2	-.8580-2	-.3274-1	-.4901-1
1.30	-.9262-1	-.2178-1	.3624-2	.3162-2	.6611-3	.2381-6	-.2258-2	-.2374-2	-.8583-2	-.3275-1	-.4903-1
1.40	-.9262-1	-.2178-1	.3624-2	.3162-2	.6609-3	.1581-7	-.2259-2	-.2375-2	-.8584-2	-.3275-1	-.4903-1

TABLE 3: RADIAL VELOCITY $\dot{G} = -U$ ($|R| = 1$)

R	+ 1	+ 1	- 1	- 1	- 1	- 1	- 1	- 1	- 1	- 1	- 1
η \ $\varkappa$	+ 10	+ 1	-.01	-.035	-.17	-.2056	-.3271	- 1/3	- 2/3	- 2	- 3
.00	0	0	0	0	0	0	0	0	0	0	0
.05	-.1189	-.2153-1	.4938-2	.4520-2	.2262-2	.1666-2	-.3699-3	-.4744-3	-.6068-2	-.2812-1	-.4373-1
.10	-.1921	-.3617-1	.7839-2	.7124-2	.3262-2	.2243-2	-.1241-2	-.1420-2	-.1099-1	-.4866-1	-.7512-1
.15	-.2277	-.4476-1	.9144-2	.8244-2	.3379-2	.2093-2	-.2297-2	-.2522-2	-.1458-1	-.6196-1	-.9498-1
.20	-.2347	-.4836-1	.9287-2	.8298-2	.2949-2	.1536-2	-.3291-2	-.3539-2	-.1680-1	-.6880-1	-.1047
.25	-.2219	-.4808-1	.8660-2	.7660-2	.2251-2	.8224-3	-.4061-2	-.4311-2	-.1773-1	-.7021-1	-.1061
.30	-.1968	-.4504-1	.7590-2	.6638-2	.1488-2	.1275-3	-.4523-2	-.4762-2	-.1754-1	-.6741-1	-.1012
.35	-.1659	-.4025-1	.6332-2	.5468-2	.7936-3	-.4417-3	-.4664-2	-.4881-2	-.1648-1	-.6165-1	-.9201-1
.40	-.1339	-.3455-1	.5065-2	.4312-2	.2383-3	-.8386-3	-.4520-2	-.4709-2	-.1482-1	-.5411-1	-.8025-1
.45	-.1039	-.2864-1	.3904-2	.3271-2	-.1543-3	-.1059-2	-.4155-2	-.4314-2	-.1282-1	-.4578-1	-.6748-1
.50	-.7775-1	-.2298-1	.2908-2	.2393-2	-.3932-3	-.1130-2	-.3649-2	-.3779-2	-.1070-1	-.3745-1	-.5489-1
.55	-.5619-1	-.1790-1	.2099-2	.1693-2	-.5058-3	-.1087-2	-.3075-2	-.3177-2	-.8644-2	-.2970-1	-.4327-1
.60	-.3929-1	-.1355-1	.1470-2	.1159-2	-.5262-3	-.9719-3	-.2496-2	-.2574-2	-.6765-2	-.2286-1	-.3313-1
.65	-.2660-1	-.9983-2	.1000-2	.7684-3	-.4876-3	-.8199-3	-.1956-2	-.2014-2	-.5139-2	-.1711-1	-.2465-1
.70	-.1744-1	-.7163-2	.6618-3	.4936-3	-.4177-3	-.6588-3	-.1483-2	-.1525-2	-.3793-2	-.1246-1	-.1785-1
.75	-.1107-1	-.5010-2	.4260-3	.3071-3	-.3369-3	-.5074-3	-.1090-2	-.1120-2	-.2723-2	-.8835-2	-.1259-1
.80	-.6814-2	-.3417-2	.2669-3	.1851-3	-.2587-3	-.3762-3	-.7780-3	-.7987-3	-.1904-2	-.6105-2	-.8660-2
.85	-.4057-2	-.2275-2	.1629-3	.1078-3	-.1904-3	-.2693-3	-.5395-3	-.5534-3	-.1296-2	-.4113-2	-.5805-2
.90	-.2337-2	-.1478-2	.9680-4	.6072-4	-.1349-3	-.1867-3	-.3639-3	-.3730-3	-.8607-3	-.2704-2	-.3797-2
.95	-.1301-2	-.9388-3	.5603-4	.3293-4	-.9237-4	-.1255-3	-.2391-3	-.2449-3	-.5573-3	-.1735-2	-.2424-2
1.00	-.6986-3	-.5825-3	.3159-4	.1714-4	-.6124-4	-.8200-4	-.1530-3	-.1567-3	-.3522-3	-.1087-2	-.1512-2
1.10	-.1790-3	-.2098-3	.9296-5	.4014-5	-.2466-4	-.3226-4	-.5828-4	-.5961-4	-.1312-3	-.3990-3	-.5498-3
1.20	-.3833-4	-.6965-4	.2485-5	.7100-6	-.8937-5	-.1149-4	-.2025-4	-.2070-4	-.4482-4	-.1345-3	-.1837-3
1.30	-.6773-5	-.2163-4	.6262-6	.6898-7	-.2960-5	-.3763-5	-.6517-5	-.6656-5	-.1423-4	-.4230-4	-.5736-4
1.40	-.1351-5	-.6549-5	.1697-6	.1612-9	-.9215-6	-.1166-5	-.2004-5	-.2046-5	-.4353-5	-.1288-4	-.1740-4

TABLE 4: PRESSURE DISTRIBUTION P ($|R| = 1$)

R	+ 1	+ 1	- 1	- 1	- 1	- 1	- 1	- 1	- 1	- 1	- 1
η \ κ	+ 10	+ 1	-.01	-.035	-.17	-.2056	-.3271	- 1/3	- 2/3	- 2	- 3
.00	-.1221+2	-.5925+2	-.3074+3	-.3422+3	-.2028+3	.3168+13	.7456+3	.7019+3	.1661+3	.4129+2	.2721+2
.05	.1697+1	-.1370+2	.6984+2	.1114+3	.4994+4	.9854+13	.6729+3	.6176+3	.8350+2	.1499+2	.8964+1
.10	.1052+2	.1810+2	.2983+3	.3810+3	.7384+4	.1228+14	.4997+3	.4474+3	.1487+2	-.4697+1	-.4471+1
.15	.1533+2	.3841+2	.4142+3	.5126+3	.7843+4	.1190+14	.2841+3	.2431+3	-.3830+2	-.1838+2	-.1361+2
.20	.1718+2	.4950+2	.4499+3	.5473+3	.7116+4	.9935+13	.6988+2	.4385+2	-.7592+2	-.2686+2	-.1906+2
.25	.1699+2	.5360+2	.4332+3	.5197+3	.5786+4	.7291+13	-.1136+3	-.1246+3	-.9905+2	-.3104+2	-.2159+2
.30	.1554+2	.5270+2	.3859+3	.4570+3	.4274+4	.4614+13	-.2508+3	-.2490+3	-.1096+3	-.3188+2	-.2184+2
.35	.1344+2	.4856+2	.3247+3	.3793+3	.2851+4	.2292+13	-.3372+3	-.3259+3	-.1102+3	-.3033+2	-.2050+2
.40	.1113+2	.4259+2	.2608+3	.3004+3	.1665+4	.5080+12	-.3766+3	-.3593+3	-.1035+3	-.2724+2	-.1819+2
.45	.8914+1	.3587+2	.2013+3	.2284+3	.7716+3	-.7045+12	-.3776+3	-.3575+3	-.9225+2	-.2332+2	-.1538+2
.50	.6946+1	.2920+2	.1501+3	.1674+3	.1620+3	-.1405+13	-.3510+3	-.3306+3	-.7852+2	-.1914+2	-.1245+2
.55	.5312+1	.2307+2	.1083+3	.1187+3	-.2062+3	-.1703+13	-.3075+3	-.2886+3	-.6421+2	-.1510+2	-.9680+1
.60	.4023+1	.1775+2	.7601+2	.8153+2	-.3905+3	-.1717+13	-.2565+3	-.2401+3	-.5061+2	-.1146+2	-.7209+1
.65	.3051+1	.1336+2	.5189+2	.5438+2	-.4482+3	-.1557+13	-.2050+3	-.1914+3	-.3852+2	-.8360+1	-.5123+1
.70	.2348+1	.9871+1	.3456+2	.3530+2	-.4285+3	-.1311+13	-.1575+3	-.1468+3	-.2834+2	-.5828+1	-.3438+1
.75	.1858+1	.7200+1	.2253+2	.2237+2	-.3689+3	-.1043+13	-.1168+3	-.1087+3	-.2014+2	-.3845+1	-.2129+1
.80	.1529+1	.5222+1	.1445+2	.1390+2	-.2952+3	-.7910+12	-.8370+2	-.7777+2	-.1380+2	-.2345+1	-.1148+1
.85	.1316+1	.3803+1	.9179+1	.8547+1	-.2232+3	-.5751+12	-.5801+2	-.5383+2	-.9088+1	-.1250+1	-.4365
.90	.1183+1	.2815+1	.5842+1	.5270+1	-.1608+3	-.4027+12	-.3890+2	-.3603+2	-.5688+1	-.4746	.6387-1
.95	.1102+1	.2146+1	.3789+1	.3333+1	-.1110+3	-.2722+12	-.2519+2	-.2329+2	-.3316+1	.5841-1	.4055
1.00	.1055+1	.1705+1	.2563+1	.2227+1	-.7364+2	-.1778+12	-.1570+2	-.1448+2	-.1711+1	.4143	.6321
1.10	.1014+1	.1246+1	.1449+1	.1296+1	-.2867+2	-.6869+11	-.5203+1	-.4743+1	.1833-1	.7915	.8704
1.20	.1003+1	.1075+1	.1111+1	.1055+1	-.9005+1	-.2269+11	-.9906	-.8411	.6912	.9353	.9602
1.30	.1004+1	.1017+1	.1020+1	.1005+1	-.1512+1	-.5616+10	.5181	.5546	.9264	.9847	.9907
1.40	.1000+1	.1000+1	.1000+1	.1000+1	.1000+1	.9808	.1000+1	.1000+1	.1000+1	.1000+1	.1000+1

TABLE 5

TANGENTIAL VELOCITY V FOR κ = .1

η	R = - .1	R = - 1	R = - 10	R = - 50	R = - 100
.00	.9000	.9000	.9000	.9000	.9000
.05	.7875	.7874	.7780	.7073	.6435
.10	.6773	.6771	.6596	.5352	.4336
.15	.5714	.5711	.5476	.3906	.2760
.20	.4716	.4713	.4442	.2732	.1613
.25	.3795	.3792	.3504	.1796	.7882-1
.30	.2961	.2958	.2672	.1062	.2020-1
.35	.2222	.2219	.1946	.4956-1	-.2089-1
.40	.1579	.1576	.1326	.6540-2	-.4912-1
.45	.1031	.1028	.8070-1	-.2552-1	-.6807-1
.50	.5730-1	.5706-1	.3802-1	-.4892-1	-.8046-1
.55	.1980-1	.1959-1	.3635-2	-.6565-1	-.8834-1
.60	-.1031-1	-.1048-1	-.2352-1	-.7735-1	-.9322-1
.65	-.3401-1	-.3414-1	-.4454-1	-.8536-1	-.9616-1
.70	-.5228-1	-.5239-1	-.6049-1	-.9072-1	-.9788-1
.75	-.6610-1	-.6618-1	-.7235-1	-.9423-1	-.9886-1
.80	-.7635-1	-.7641-1	-.8100-1	-.9648-1	-.9940-1
.85	-.8379-1	-.8383-1	-.8718-1	-.9790-1	-.9969-1
.90	-.8909-1	-.8912-1	-.9150-1	-.9877-1	-.9985-1
.95	-.9279-1	-.9281-1	-.9447-1	-.9929-1	-.9993-1
1.00	-.9532-1	-.9534-1	-.9647-1	-.9960-1	-.9997-1
1.10	-.9814-1	-.9814-1	-.9864-1	-.9988-1	-.9999-1
1.20	-.9931-1	-.9931-1	-.9951-1	-.9997-1	-.9999-1
1.30	-.9976-1	-.9976-1	-.9984-1	-.9999-1	
1.40	-.9992-1	-.9993-1	-.9995-1	-.9999-1	

TABLE 6

AXIAL VELOCITY $G = w_\infty W/2\Omega\ell$ FOR $\varkappa = -.1$

η	R = - .1	R = - 1	R = - 10	R = - 50	R = - 100
.00	0	0	0	0	0
.05	.9346-5	.9334-4	.8624-3	.2577-2	.3519-2
.10	.3171-4	.3167-3	.2893-2	.7914-2	.9911-2
.15	.6009-4	.6001-3	.5424-2	.1361-1	.1570-1
.20	.8947-4	.8935-3	.7992-2	.1848-1	.1980-1
.25	.1166-3	.1165-2	.1031-1	.2213-1	.2223-1
.30	.1398-3	.1396-2	.1225-1	.2457-1	.2342-1
.35	.1583-3	.1580-2	.1376-1	.2605-1	.2384-1
.40	.1722-3	.1719-2	.1486-1	.2683-1	.2384-1
.45	.1821-3	.1818-2	.1562-1	.2715-1	.2366-1
.50	.1887-3	.1884-2	.1611-1	.2722-1	.2344-1
.55	.1929-3	.1925-2	.1640-1	.2715-1	.2324-1
.60	.1953-3	.1950-2	.1656-1	.2704-1	.2309-1
.65	.1966-3	.1962-2	.1663-1	.2692-1	.2297-1
.70	.1971-3	.1967-2	.1665-1	.2681-1	.2290-1
.75	.1972-3	.1968-2	.1664-1	.2673-1	.2285-1
.80	.1972-3	.1968-2	.1663-1	.2668-1	.2282-1
.85	.1970-3	.1966-2	.1661-1	.2664-1	.2280-1
.90	.1968-3	.1964-2	.1660-1	.2661-1	.2279-1
.95	.1966-3	.1963-2	.1658-1	.2659-1	.2278-1
1.00	.1965-3	.1962-2	.1657-1	.2659-1	.2278-1
1.10	.1964-3	.1960-2	.1656-1	.2658-1	.2278-1
1.20	.1963-3	.1959-2	.1656-1	.2657-1	.2277-1
1.30	.1963-3	.1959-2	.1656-1	.2657-1	
1.40	.1963-3	.1959-2	.1655-1	.2657-1	

TABLE 7

RADIAL VELOCITY $\dot{G} = -U$ FOR $\varkappa = -.1$

η	R = - .1	R = - 1	R = - 10	R = - 50	R = - 100
.00	0	0	0	0	0
.05	.3438-3	.3434-2	.3153-1	.8963-1	.1162
.10	.5273-3	.5267-2	.4748-1	.1160	.1285
.15	.5912-3	.5904-2	.5221-1	.1081	.1000
.20	.5735-3	.5725-2	.4959-1	.8558-1	.6417-1
.25	.5068-3	.5058-2	.4285-1	.6036-1	.3464-1
.30	.4171-3	.4161-2	.3441-1	.3833-1	.1470-1
.35	.3228-3	.3220-2	.2593-1	.2164-1	.3187-2
.40	.2360-3	.2353-2	.1839-1	.1030-1	-.2373-2
.45	.1629-3	.1624-2	.1225-1	.3373-2	-.4307-2
.50	.1057-3	.1053-2	.7610-2	-.3629-3	-.4345-2
.55	.6384-4	.6357-3	.4326-2	-.2015-2	-.3594-2
.60	.3505-4	.3485-3	.2160-2	-.2449-2	-.2662-2
.65	.1657-4	.1645-3	.8359-3	-.2264-2	-.1834-2
.70	.5614-5	.5548-4	.1029-3	-.1833-2	-.1199-2
.75	-.2145-6	-.2487-5	-.2464-3	-.1364-2	-.7563-3
.80	-.2812-5	-.2826-4	-.3668-3	-.9535-3	-.4643-3
.85	-.3547-5	-.3550-4	-.3652-3	-.6342-3	-.2799-3
.90	-.3333-5	-.3331-4	-.3092-3	-.4044-3	-.1665-3
.95	-.2732-5	-.2729-4	-.2381-3	-.2487-3	-.9794-4
1.00	-.2057-5	-.2052-4	-.1714-3	-.1481-3	-.5689-4
1.10	-.9792-6	-.9765-5	-.7657-4	-.4852-4	-.1855-4
1.20	-.3938-6	-.3925-5	-.2942-4	-.1480-4	-.6189-5
1.30	-.1391-6	-.1386-5	-.1006-4	-.4467-5	
1.40	-.4443-7	-.4426-6	-.3169-5	-.1391-5	

TABLE 8

PRESSURE DISTRIBUTION P FOR α = - .1

η	R = - .1	R = - 1	R = - 10	R = - 50	R = - 100
.00	-.4733+5	-.4740+3	-.5352+1	-.4555	-.1867
.05	.4220+5	.4240+3	.6198+1	.2102+1	.2087+1
.10	.9162+5	.9194+3	.1228+2	.2974+1	.2525+1
.15	.1119+6	.1123+4	.1454+2	.3004+1	.2318+1
.20	.1126+6	.1130+4	.1436+2	.2684+1	.1962+1
.25	.1017+6	.1019+4	.1282+2	.2272+1	.1632+1
.30	.8495+5	.8518+3	.1067+2	.1885+1	.1377+1
.35	.6671+5	.6689+3	.8434+1	.1572+1	.1204+1
.40	.4958+5	.4973+3	.6400+1	.1342+1	.1096+1
.45	.3497+5	.3510+3	.4714+1	.1187+1	.1037+1
.50	.2340+5	.2351+3	.3415+1	.1089+1	.1008+1
.55	.1479+5	.1489+3	.2475+1	.1033+1	.9962
.60	.8761+4	.8856+2	.1835+1	.1004+1	.9933
.65	.4773+4	.4867+2	.1426+1	.9921	.9939
.70	.2299+4	.2393+2	.1182+1	.9886	.9956
.75	.8739+3	.9686+1	.1049+1	.9893	.9972
.80	.1301+3	.2259+1	.9849	.9915	.9984
.85	-.2016+3	-.1048+1	.9608	.9939	.9991
.90	-.3047+3	-.2071+1	.9575	.9959	.9996
.95	-.2950+3	-.1969+1	.9633	.9975	.9998
1.00	-.2406+3	-.1421+1	.9719	.9985	.9999
1.10	-.1209+3	-.2206	.9869	.9996	.1000+1
1.20	-.4616+2	.5282	.9952	.9999	.1000+1
1.30	-.1193+2	.8707	.9987	.9999	
1.40	-.1000+1	.1000+1	.1000+1	.1000+1	

TABLE 9

TANGENTIAL VELOCITY V FOR $\kappa = -.22$

η	R = - .1	R = - 1	R = - 10	R = - 30	R = - 50
.00	.7800	.7800	.7800	.7800	.7800
.05	.6675	.6675	.6654	.6548	.6670
.10	.5573	.5573	.5536	.5356	.5664
.15	.4514	.4513	.4467	.4254	.4816
.20	.3516	.3516	.3466	.3251	.4106
.25	.2595	.2594	.2545	.2347	.3494
.30	.1761	.1761	.1715	.1542	.2942
.35	.1022	.1022	.9795-1	.8329-1	.2421
.40	.3790-1	.3786-1	.3414-1	.2188-1	.1915
.45	-.1690-1	-.1694-1	-.2017-1	-.3038-1	.1419
.50	-.6270-1	-.6273-1	-.6547-1	-.7397-1	.9361-1
.55	-.1002	-.1002	-.1025	-.1095	.4735-1
.60	-.1303	-.1303	-.1322	-.1380	.3954-2
.65	-.1540	-.1540	-.1555	-.1602	-.3577-1
.70	-.1723	-.1723	-.1735	-.1772	-.7121-1
.75	-.1861	-.1861	-.1870	-.1899	-.1021
.80	-.1963	-.1964	-.1970	-.1992	-.1282
.85	-.2038	-.2038	-.2043	-.2059	-.1499
.90	-.2091	-.2091	-.2094	-.2106	-.1674
.95	-.2128	-.2128	-.2130	-.2138	-.1813
1.00	-.2153	-.2153	-.2155	-.2160	-.1920
1.10	-.2181	-.2181	-.2182	-.2184	-.2061
1.20	-.2193	-.2193	-.2193	-.2194	-.2136
1.30	-.2198	-.2198	-.2198	-.2198	-.2173
1.40	-.2199	-.2199	-.2199	-.2199	-.2190

TABLE 10

AXIAL VELOCITY $G = w_\infty W/2\Omega\ell$ FOR $\varkappa = -.22$

η	R = - .1	R = - 1	R = - 10	R = - 30	R = - 50
.00	0	0	0	0	0
.05	.4068-5	.4067-4	.3970-3	.1046-2	.1767-2
.10	.1256-4	.1255-3	.1219-2	.3106-2	.5238-2
.15	.2128-4	.2127-3	.2051-2	.5017-2	.8373-2
.20	.2772-4	.2771-3	.2650-2	.6136-2	.9946-2
.25	.3076-4	.3074-3	.2909-2	.6224-2	.9368-2
.30	.3027-4	.3024-3	.2819-2	.5319-2	.6522-2
.35	.2678-4	.2676-3	.2437-2	.3623-2	.1613-2
.40	.2117-4	.2114-3	.1851-2	.1409-2	-.4958-2
.45	.1435-4	.1432-3	.1152-2	-.1048-2	-.1269-1
.50	.7156-5	.7125-4	.4223-3	-.3514-2	-.2105-1
.55	.2428-6	.2112-5	-.2743-3	-.5813-2	-.2955-1
.60	-.5964-5	-.5995-4	-.8966-3	-.7837-2	-.3777-1
.65	-.1124-4	-.1127-3	-.1423-2	-.9532-2	-.4540-1
.70	-.1551-4	-.1554-3	-.1849-2	-.1089-1	-.5222-1
.75	-.1883-4	-.1886-3	-.2179-2	-.1195-1	-.5810-1
.80	-.2132-4	-.2135-3	-.2426-2	-.1273-1	-.6302-1
.85	-.2312-4	-.2315-3	-.2604-2	-.1330-1	-.6701-1
.90	-.2438-4	-.2441-3	-.2729-2	-.1370-1	-.7015-1
.95	-.2524-4	-.2527-3	-.2813-2	-.1397-1	-.7256-1
1.00	-.2581-4	-.2584-3	-.2869-2	-.1414-1	-.7436-1
1.10	-.2640-4	-.2643-3	-.2927-2	-.1433-1	-.7658-1
1.20	-.2661-4	-.2665-3	-.2949-2	-.1440-1	-.7764-1
1.30	-.2669-4	-.2672-3	-.2957-2	-.1443-1	-.7809-1
1.40	-.2672-4	-.2675-3	-.2959-2	-.1443-1	-.7826-1

TABLE 11

RADIAL VELOCITY $\dot{G} = -U$ FOR $\varkappa = +.22$

η	R = - .1	R = - 1	R = - 10	R = - 30	R = - 50
.00	0	0	0	0	0
.05	.1426-3	.1425-2	.1387-1	.3592-1	.6070-1
.10	.1831-3	.1830-2	.1762-1	.4265-1	.7140-1
.15	.1575-3	.1574-2	.1488-1	.3168-1	.4998-1
.20	.9660-4	.9650-3	.8737-2	.1232-1	.1101-1
.25	.2451-4	.2442-3	.1581-2	-.8637-2	-.3447-1
.30	-.4224-4	-.4232-3	-.4968-2	-.2685-1	-.7864-1
.35	-.9411-4	-.9418-3	-.9994-2	-.4004-1	-.1164
.40	-.1274-3	-.1275-2	-.1316-1	-.4759-1	-.1447
.45	-.1426-3	-.1426-2	-.1453-1	-.4992-1	-.1626
.50	-.1428-3	-.1428-2	-.1443-1	-.4812-1	-.1702
.55	-.1323-3	-.1323-2	-.1329-1	-.4349-1	-.1685
.60	-.1152-3	-.1152-2	-.1153-1	-.3728-1	-.1595
.65	-.9544-4	-.9544-3	-.9519-2	-.3054-1	-.1450
.70	-.7565-4	-.7564-3	-.7525-2	-.2403-1	-.1272
.75	-.5765-4	-.5764-3	-.5722-2	-.1822-1	-.1080
.80	-.4238-4	-.4238-3	-.4199-2	-.1336-1	-.8887-1
.85	-.3014-4	-.3014-3	-.2981-2	-.9486-2	-.7100-1
.90	-.2077-4	-.2077-3	-.2051-2	-.6536-2	-.5512-1
.95	-.1390-4	-.1390-3	-.1371-2	-.4375-2	-.4163-1
1.00	-.9043-5	-.9042-4	-.8908-3	-.2850-2	-.3060-1
1.10	-.3535-5	-.3534-4	-.3475-3	-.1118-2	-.1526-1
1.20	-.1253-5	-.1253-4	-.1230-3	-.3979-3	-.6840-2
1.30	-.4090-6	-.4089-5	-.4008-4	-.1303-3	-.2730-2
1.40	-.1266-6	-.1265-5	-.1239-4	-.4039-4	-.9338-3

TABLE 12

PRESSURE DISTRIBUTION P FOR κ = - .22

η	R = - .1	R = - 1	R = - 10	R = - 30	R = - 50
.00	.1610+7	.1606+5	.1341+3	.6718+1	.6854
.05	.3614+7	.3606+5	.2931+3	.1249+2	.8849
.10	.4218+7	.4208+5	.3389+3	.1371+2	.9272
.15	.3920+7	.3910+5	.3126+3	.1218+2	.8693
.20	.3130+7	.3122+5	.2475+3	.9266+1	.7502
.25	.2157+7	.2151+5	.1686+3	.5927+1	.5981
.30	.1214+7	.1210+5	.9252+2	.2802+1	.4362
.35	.4231+6	.4215+4	.2917+2	.2631	.2855
.40	-.1617+6	-.1619+4	-.1734+2	-.1530+1	.1642
.45	-.5374+6	-.5365+4	-.4685+2	-.2576+1	.8516-1
.50	-.7317+6	-.7303+4	-.6170+2	-.2984+1	.5467-1
.55	-.7870+6	-.7854+4	-.6536+2	-.2912+1	.7194-1
.60	-.7483+6	-.7466+4	-.6151+2	-.2529+1	.1302
.65	-.6553+6	-.6539+4	-.5340+2	-.1987+1	.2188
.70	-.5394+6	-.5382+4	-.4357+2	-.1399+1	.3254
.75	-.4220+6	-.4210+4	-.3374+2	-.8423	.4385
.80	-.3161+6	-.3153+4	-.2494+2	-.3600	.5485
.85	-.2276+6	-.2270+4	-.1763+2	.3166-1	.6486
.90	-.1582+6	-.1577+4	-.1191+2	.3333	.7349
.95	-.1063+6	-.1059+4	-.7657+1	.5553	.8060
1.00	-.6910+5	-.6884+3	-.4619+1	.7125	.8623
1.10	-.2647+5	-.2631+3	-.1146+1	.8906	.9368
1.20	-.8696+4	-.8576+2	.2968	.9642	.9752
1.30	-.2142+4	-.2038+2	.8270	.9912	.9928
1.40	.1000+1	.1000+1	.1000+1	.1000+1	.1000+1

APPENDIX B

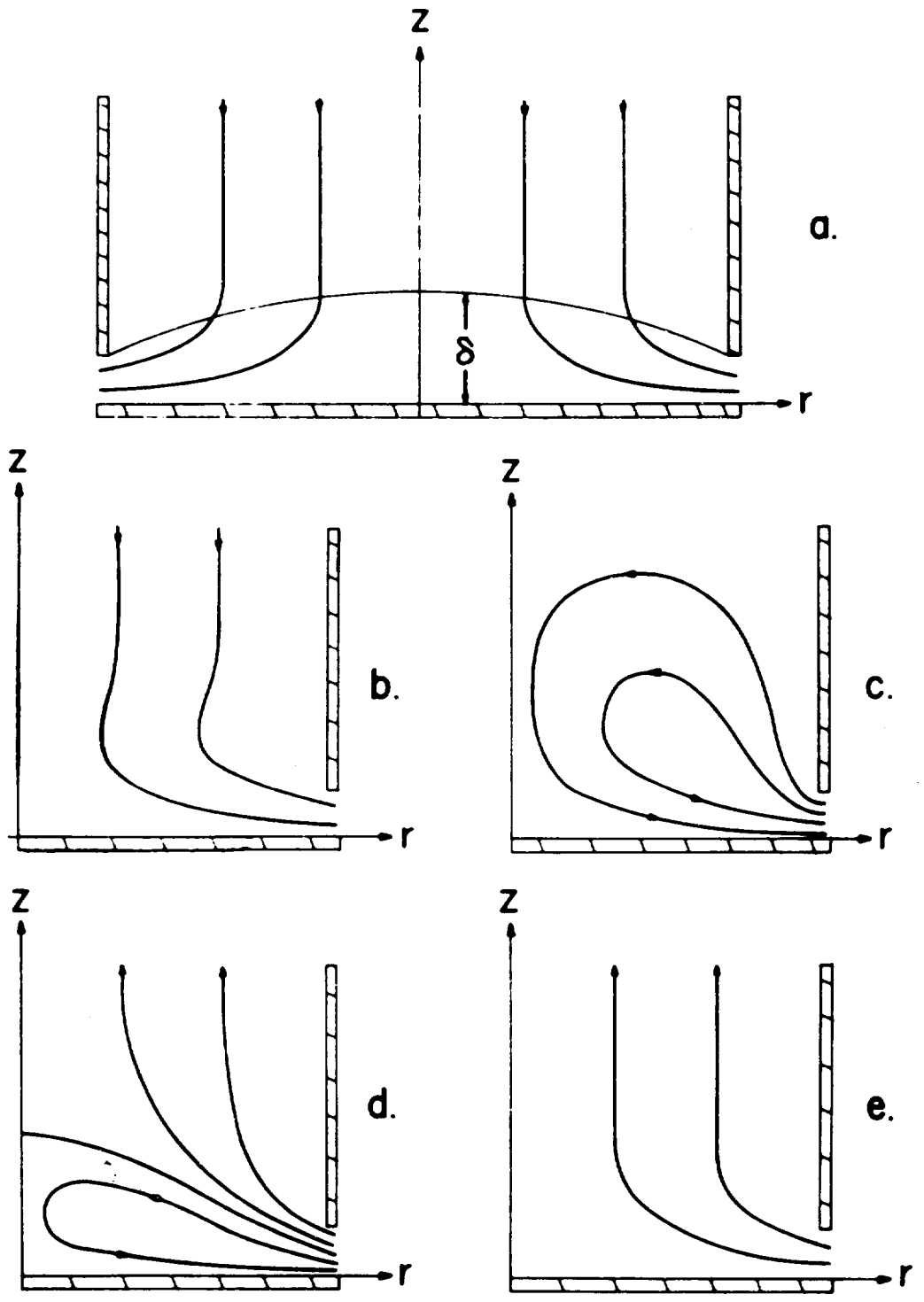

Fig. 1: a. Pure Stagnation Flow,
b. Distorted Stagnation Flow, c. Limiting Cell Flow,
d. Cell Flow, e. Pure Wake Flow.

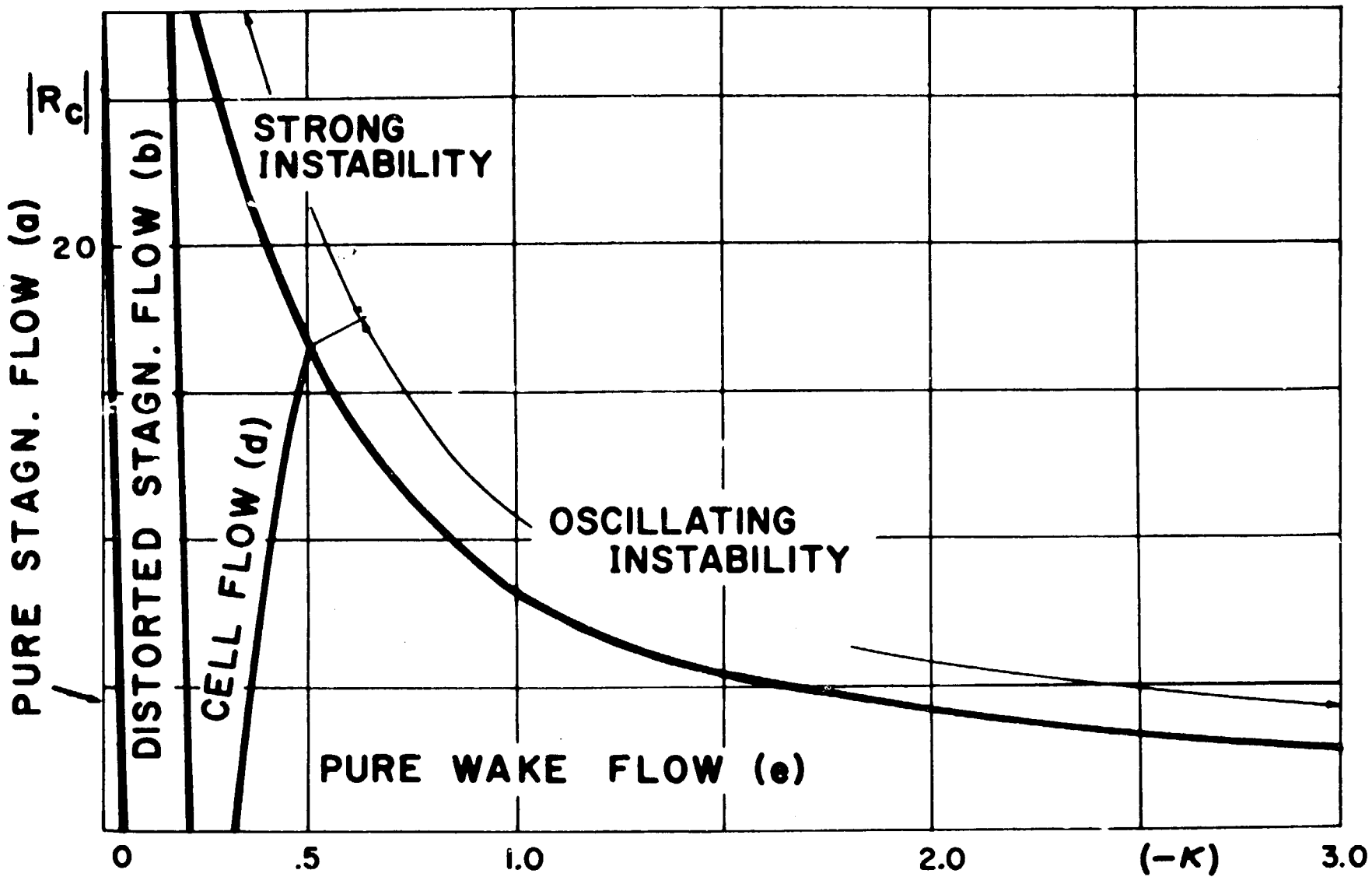

Fig. 2: Critical Reynolds number $|R_c|$ versus velocity ratio (- κ)

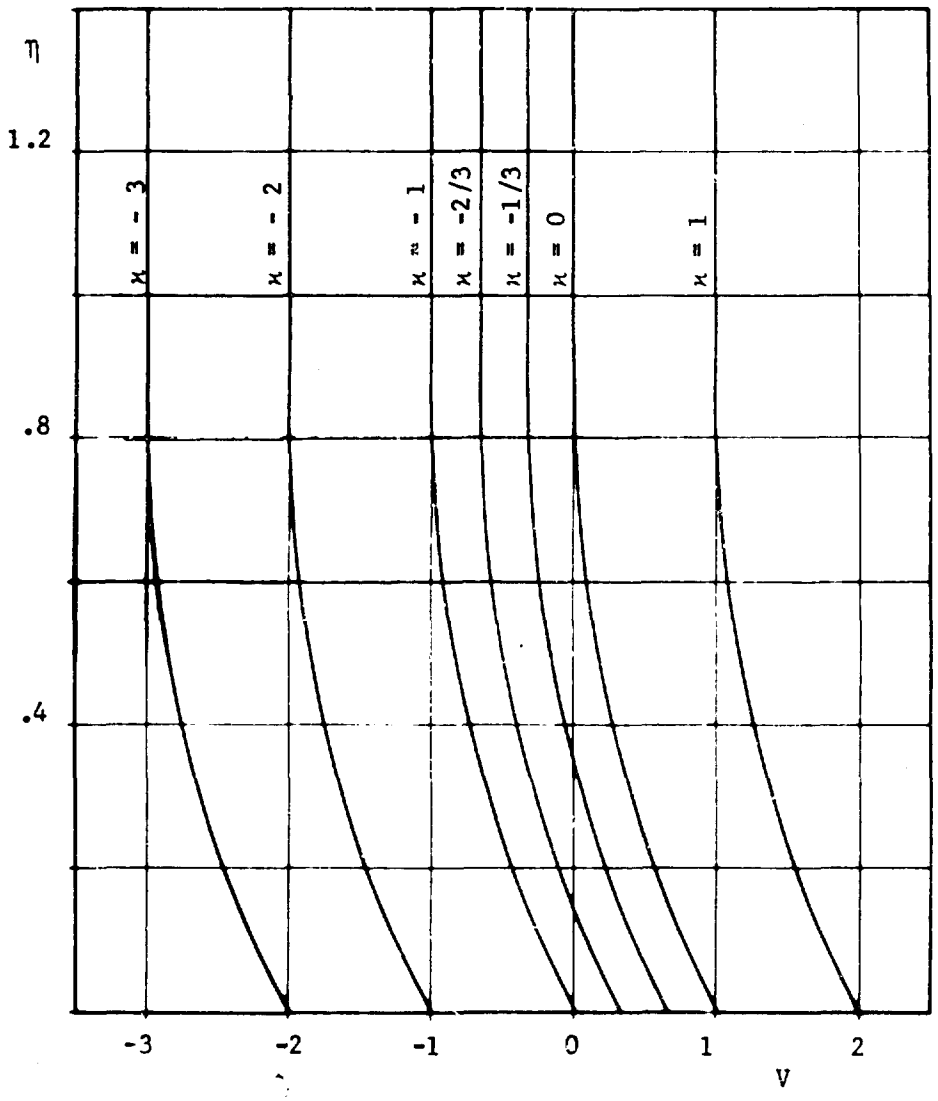

Fig. 3a: Tangential velocities V versus dimensionless variable η at Reynolds number $|R| = 1$ and different velocity ratios κ.

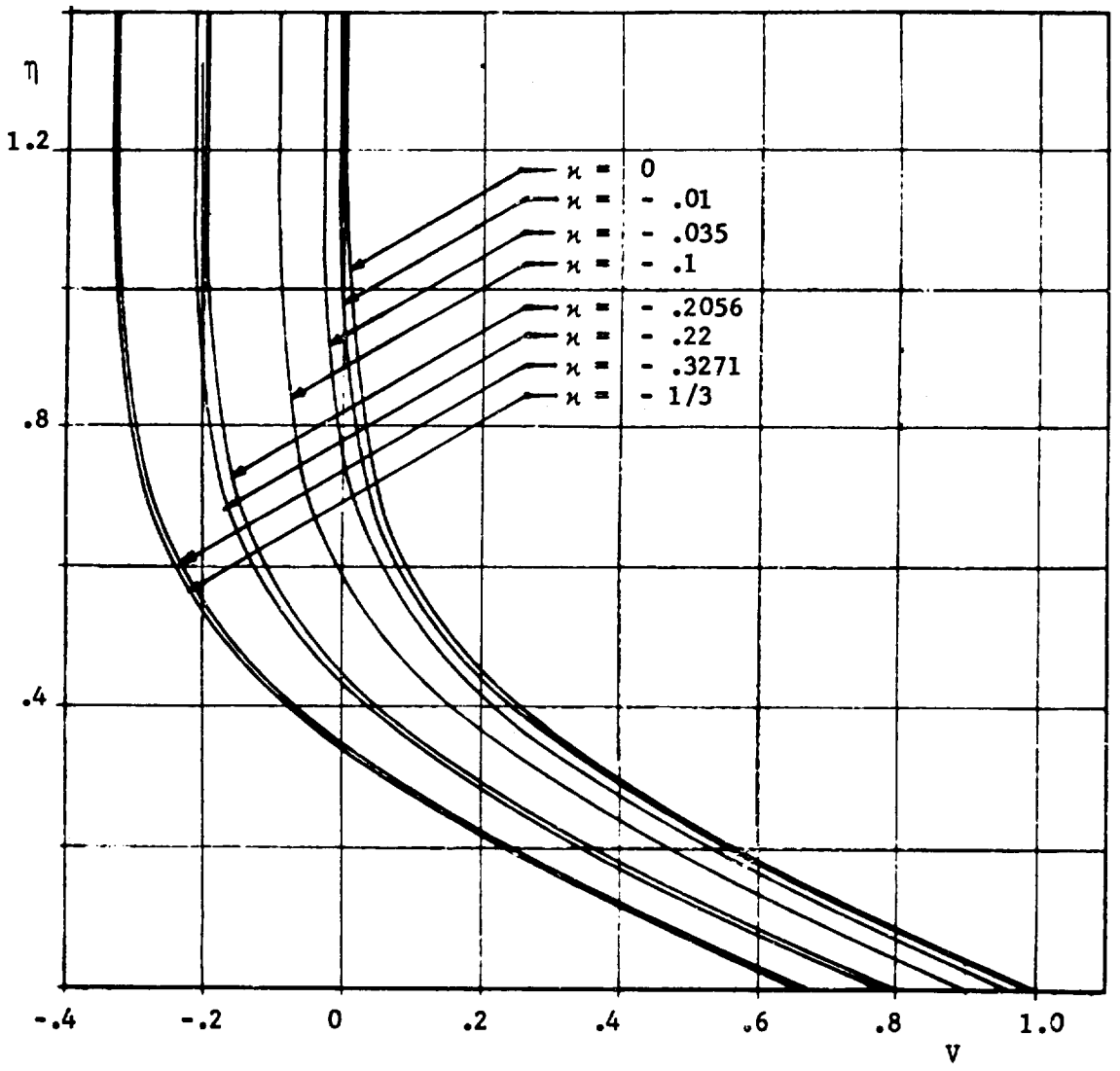

Fig. 3b: Tangential velocities V versus dimensionless variable η at Reynolds number $|R| = 1$ and different velocity ratios κ.

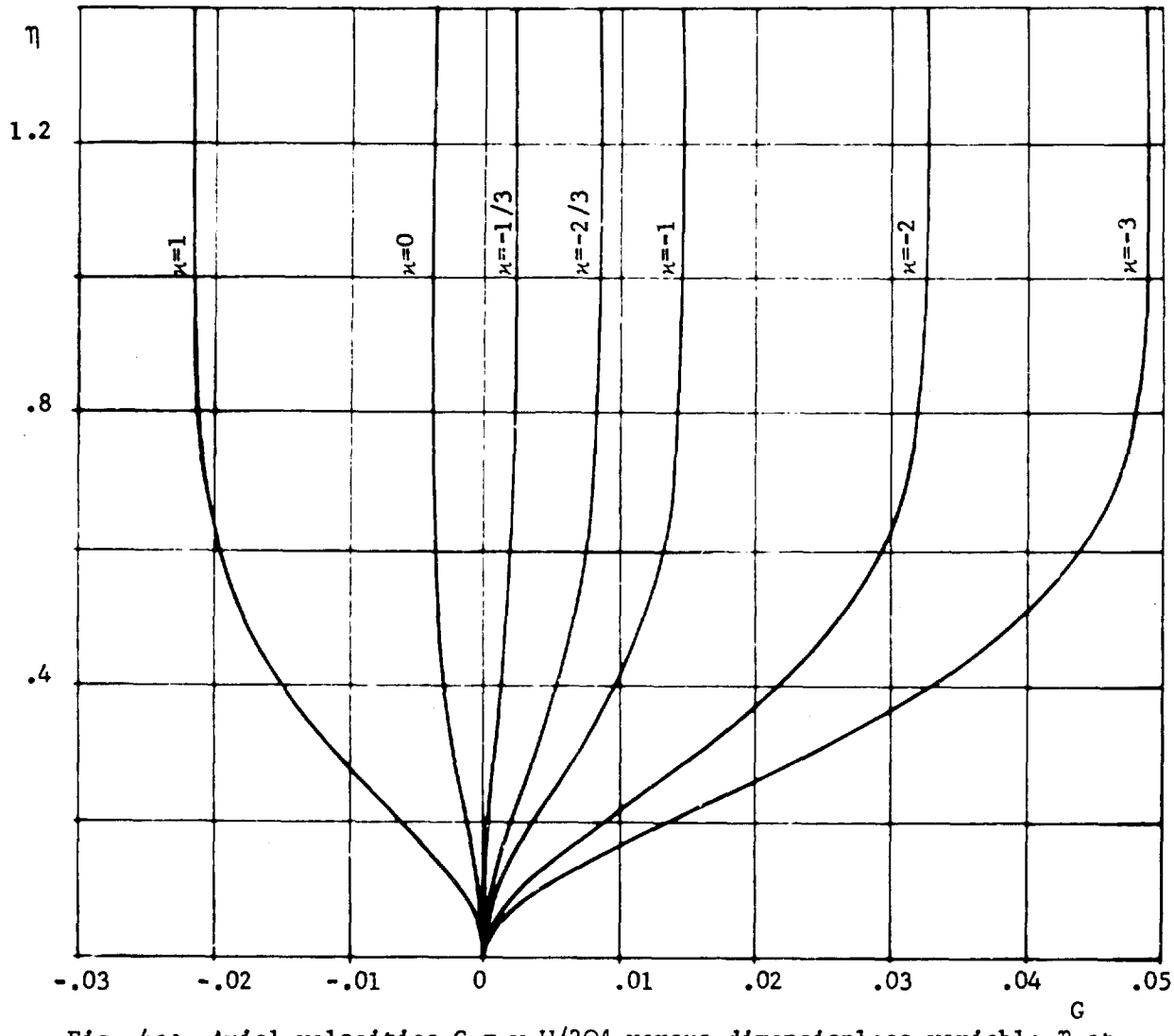

Fig. 4a: Axial velocities $G = w_\infty W/2\Omega\ell$ versus dimensionless variable η at Reynolds number $|R| = 1$ and different velocity ratios κ.

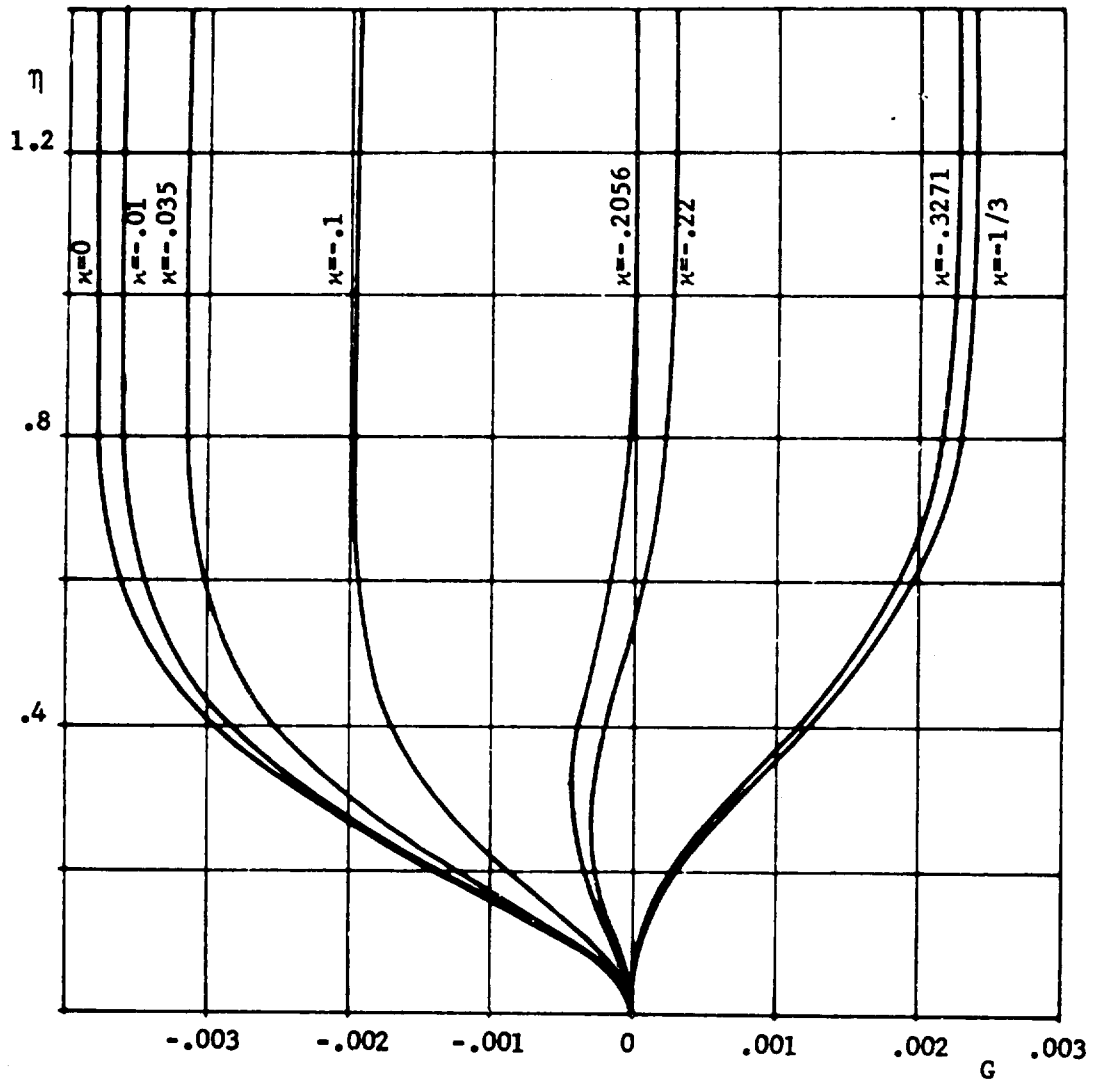

Fig. 4b: Axial velocities $G = w_\infty W/2\Omega\ell$ versus dimensionless variable η at Reynolds number $|R| = 1$ and different velocity ratios $\varkappa$.

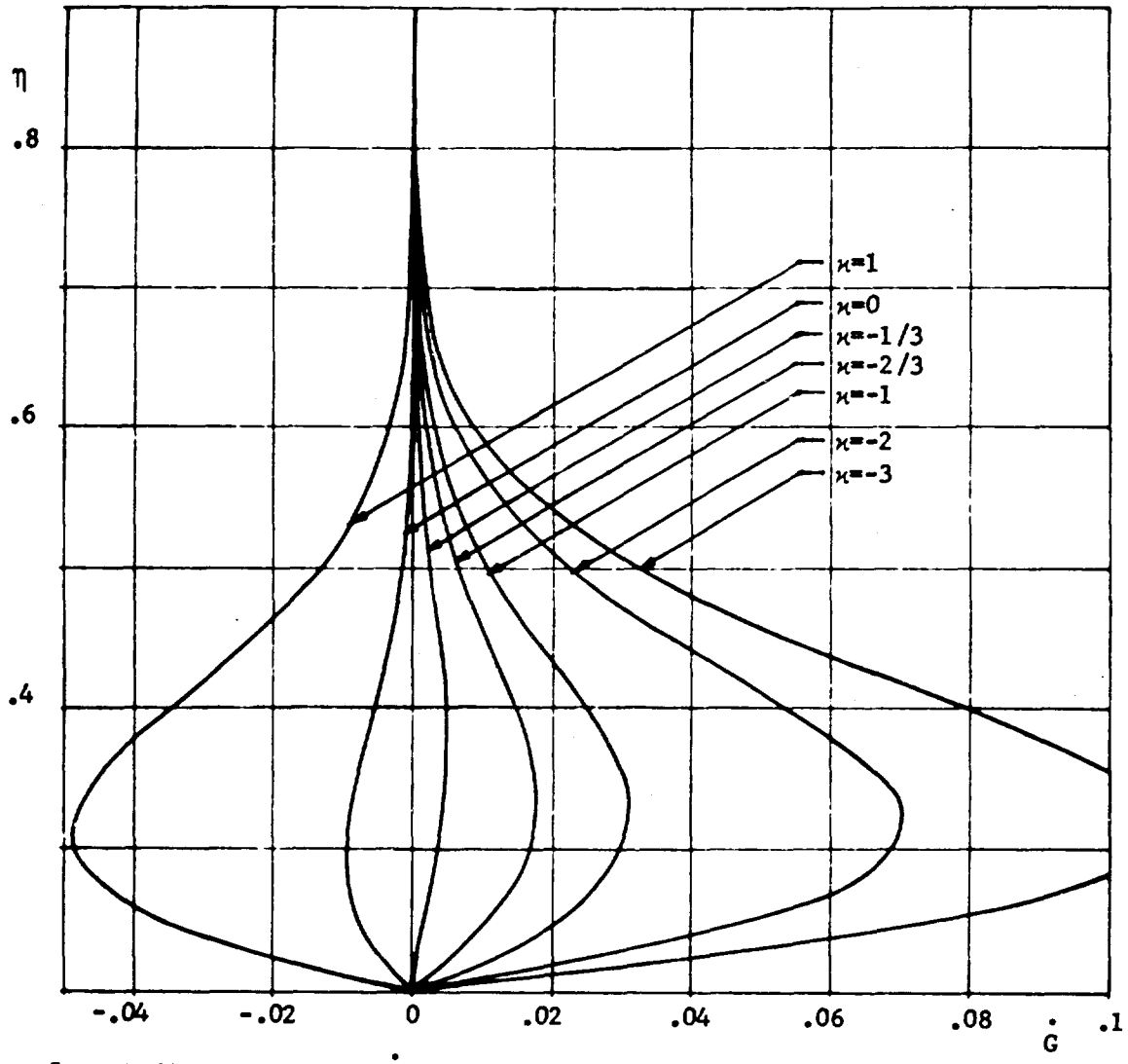

Fig. 5a: Radial velocities $\dot{G} = -U$ versus dimensionless variable η at Reynolds number $|R| = 1$ and different velocity ratios κ.

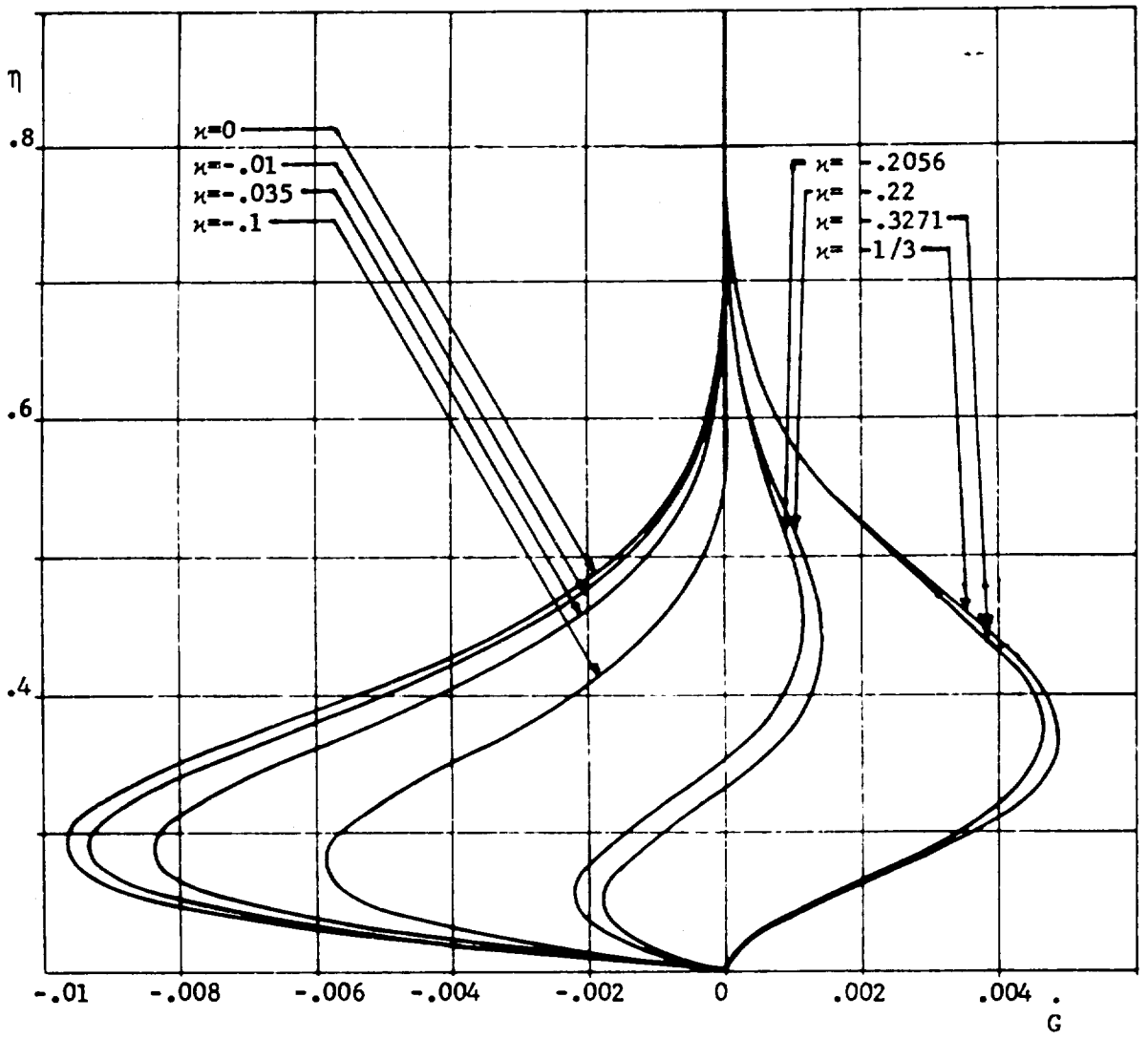

Fig. 5b: Radial velòcities $\dot{G} = -U$ versus dimensionless variable η at Reynolds number $|R| = 1$ and different velocity ratios κ.

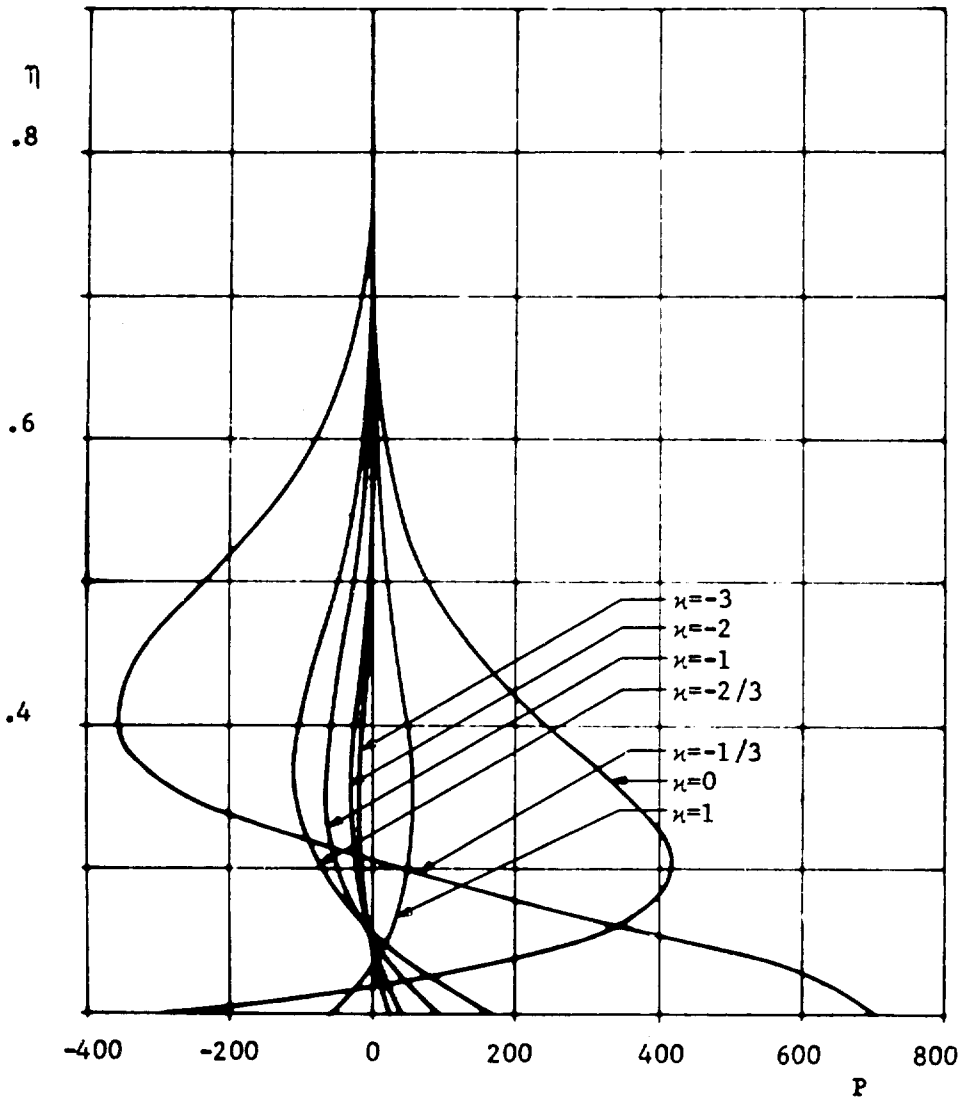

Fig. 6a: Pressure functions P versus dimensionless variable η at Reynolds number $|R| = 1$ and different velocity ratios κ.

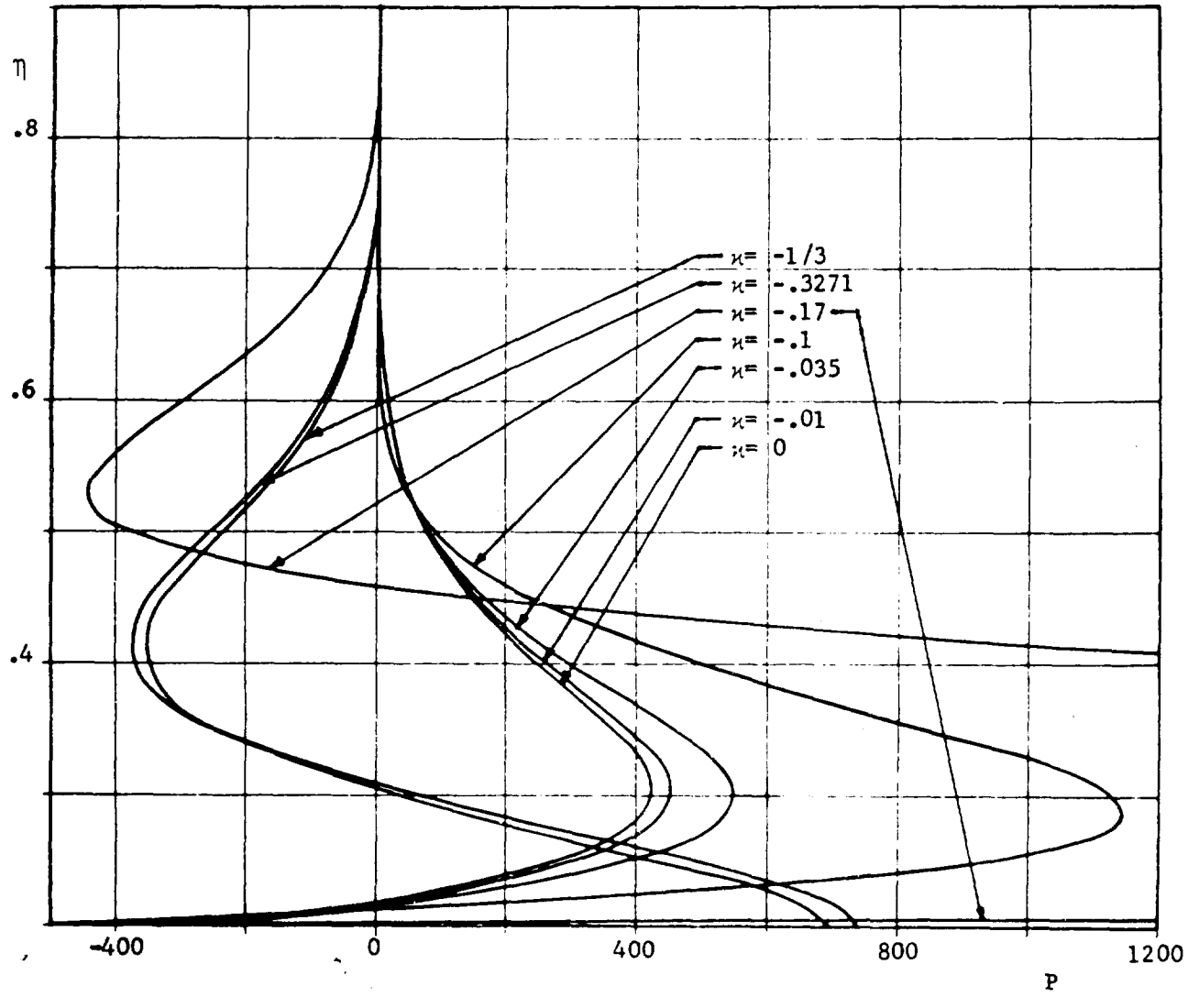

Fig. 6b: Pressure functions P versus dimensionless variable η at Reynolds number $|R| = 1$ and different velocity ratios κ.

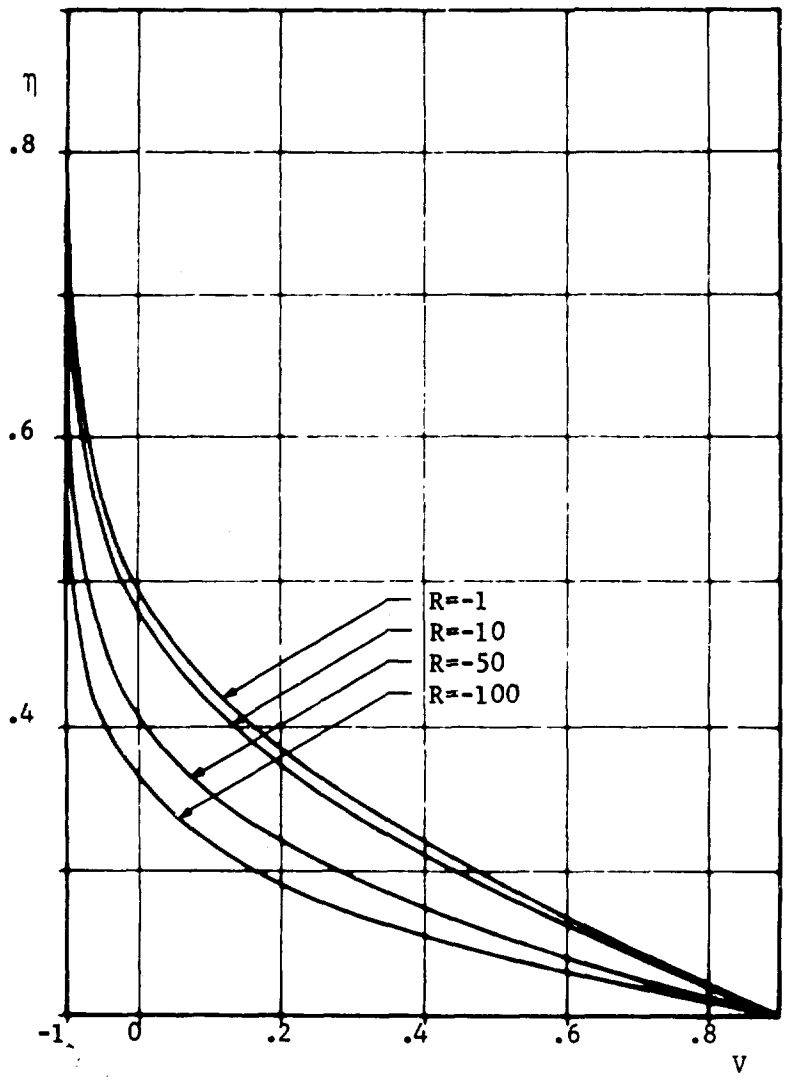

Fig. 7: Tangential velocities V versus dimensionless variable η at velocity ratio $\varkappa$ = - .1 and different Reynolds numbers R.

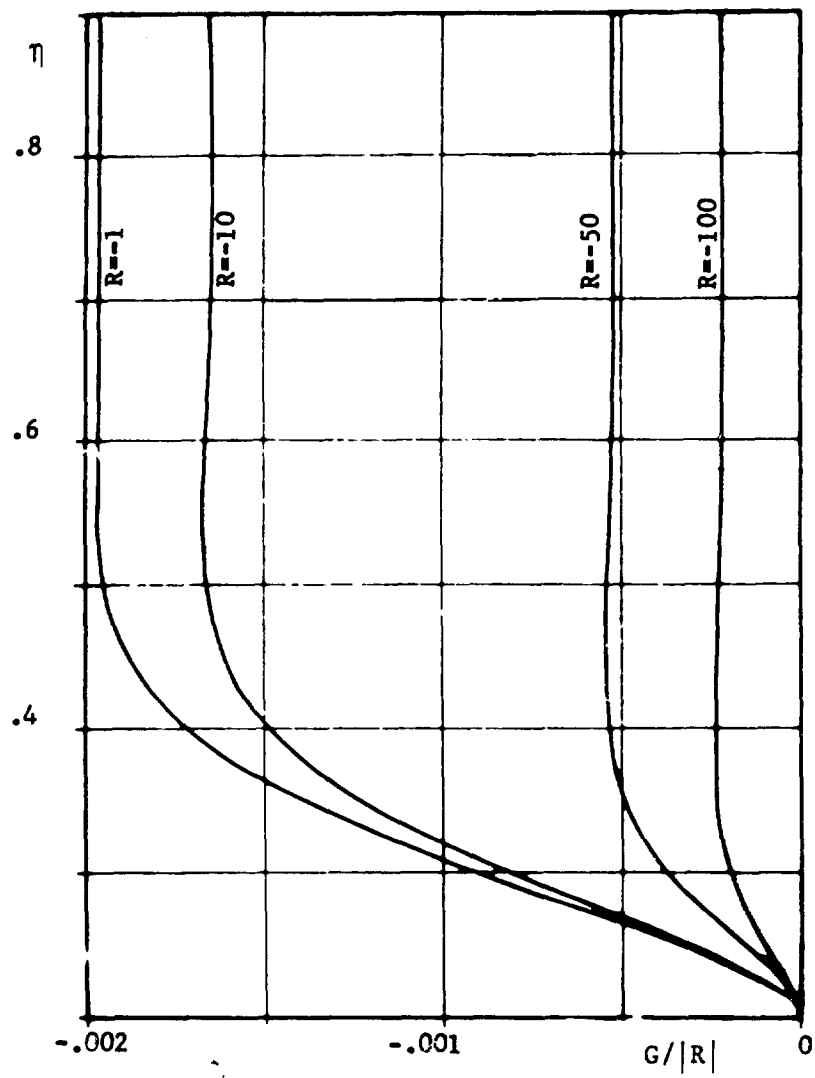

Fig. 8: Axial velocities $G = w_\infty W/2\Omega\ell$ versus dimensionless variable η at velocity ratio $\varkappa = -.1$ and different Reynolds numbers R.

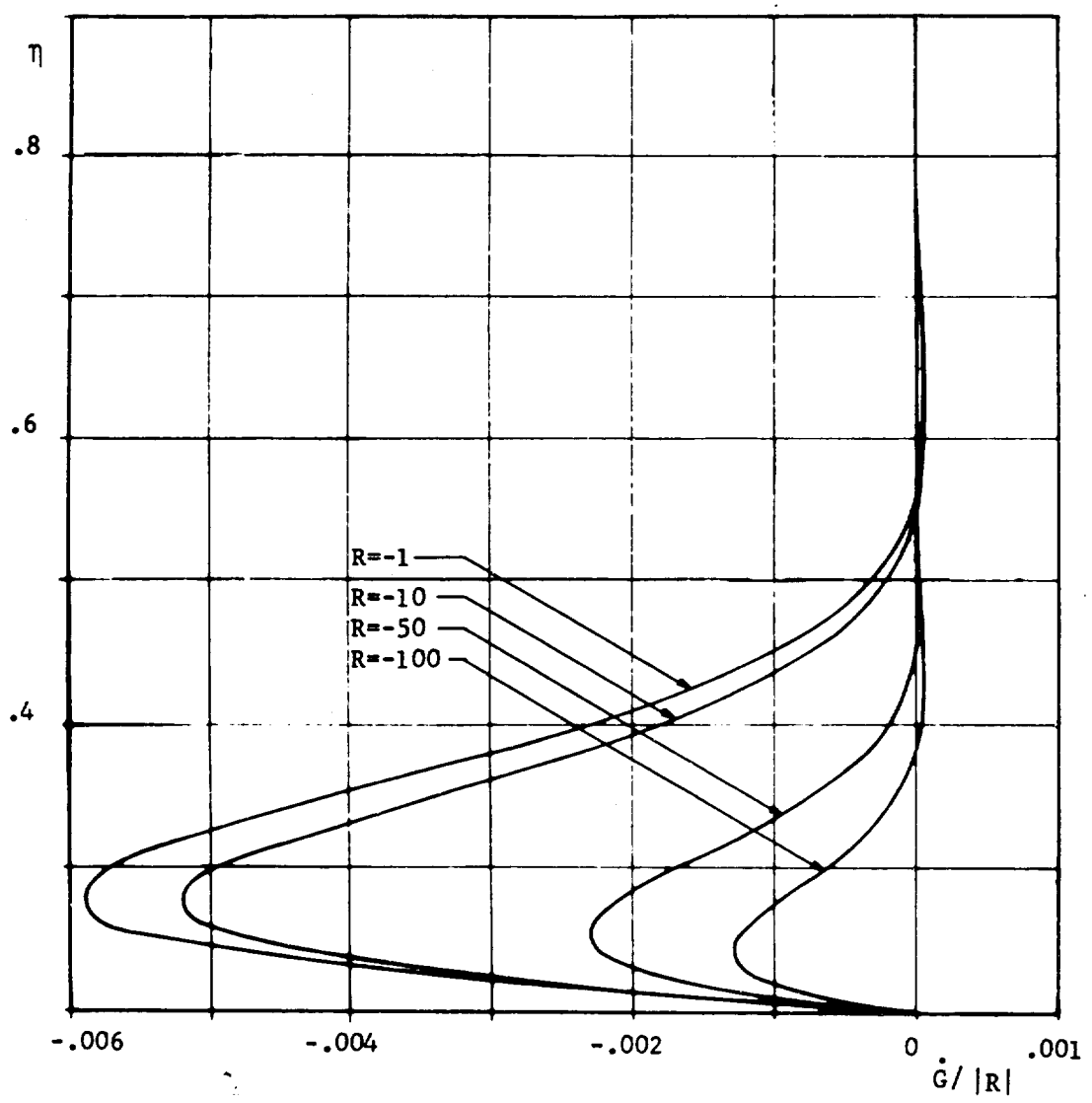

Fig. 9: Radial velocities $\dot{G} = -U$ versus dimensionless variable η at velocity ratio $\varkappa = -.1$ and different Reynolds numbers R.

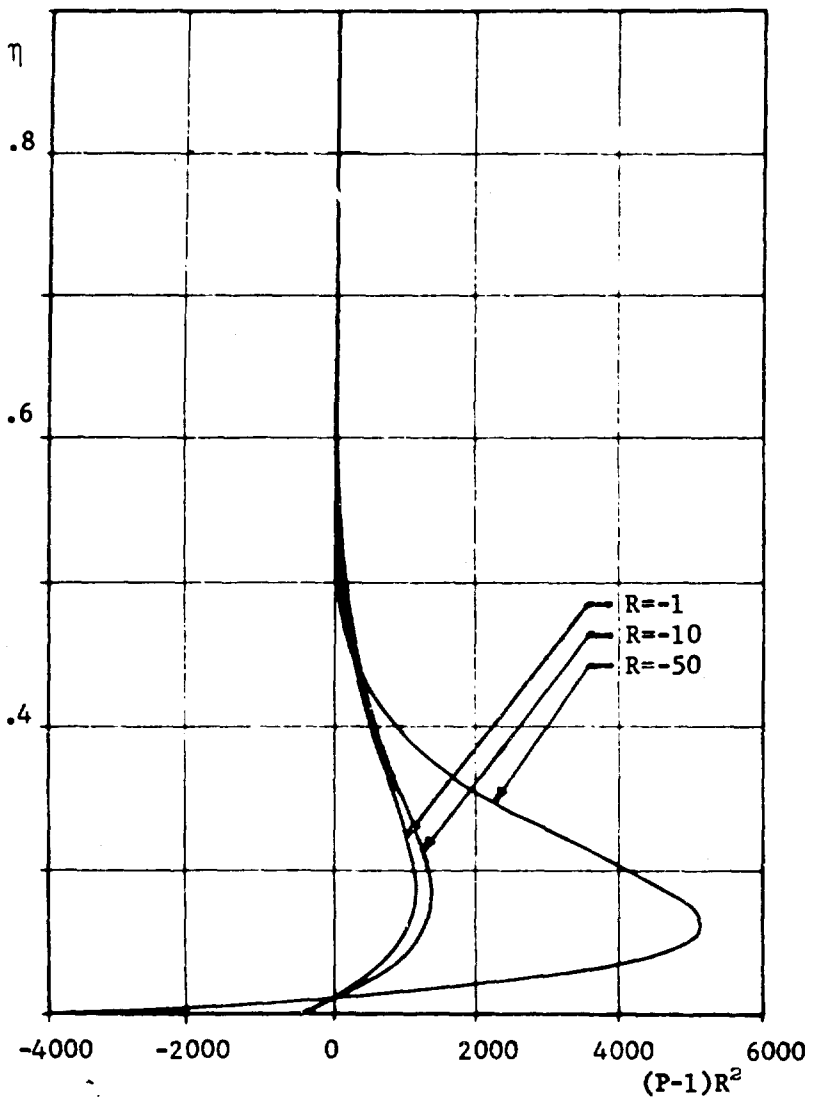

Fig. 10: Pressure functions P versus dimensionless variable η at velocity ratio $\varkappa = -.1$ and different Reynolds numbers R.

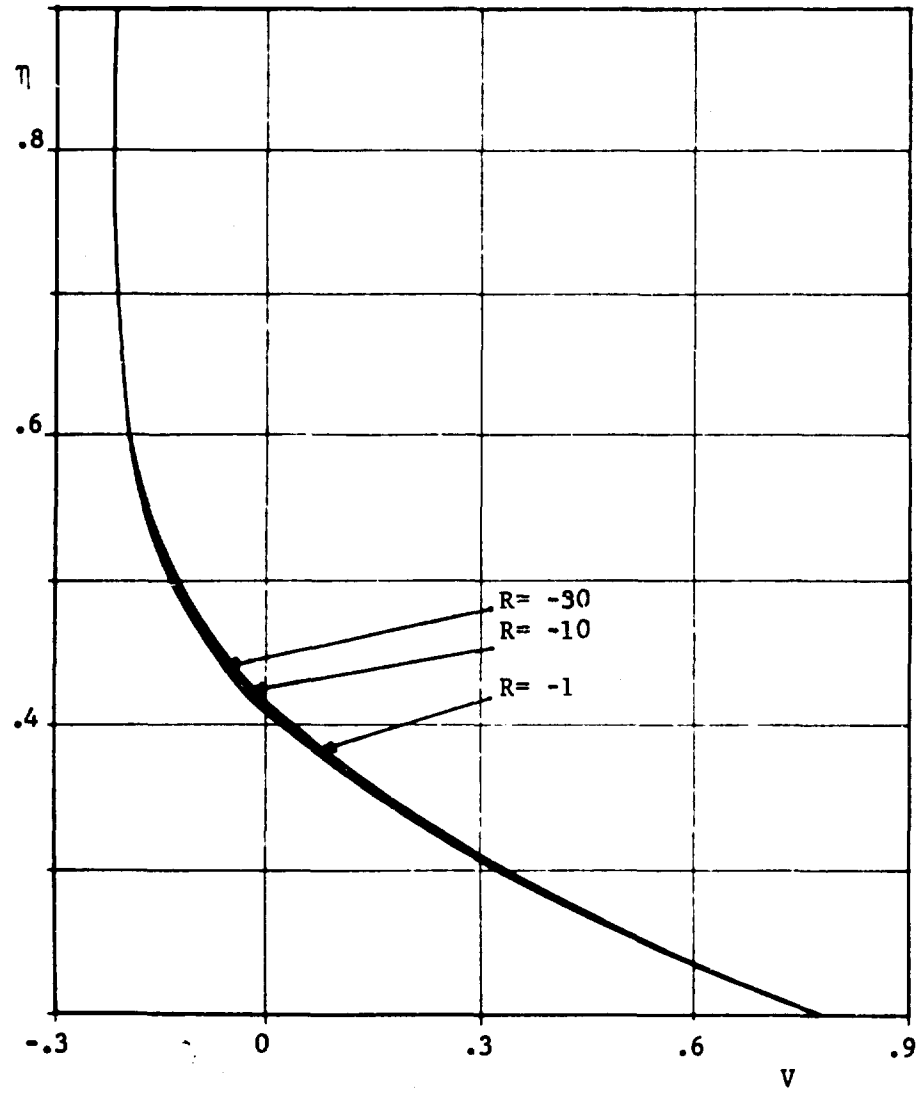

Fig. 11: Tangential velocities V versus dimensionless variable η at velocity ratio $\varkappa$ = - .22 and different Reynolds numbers R.

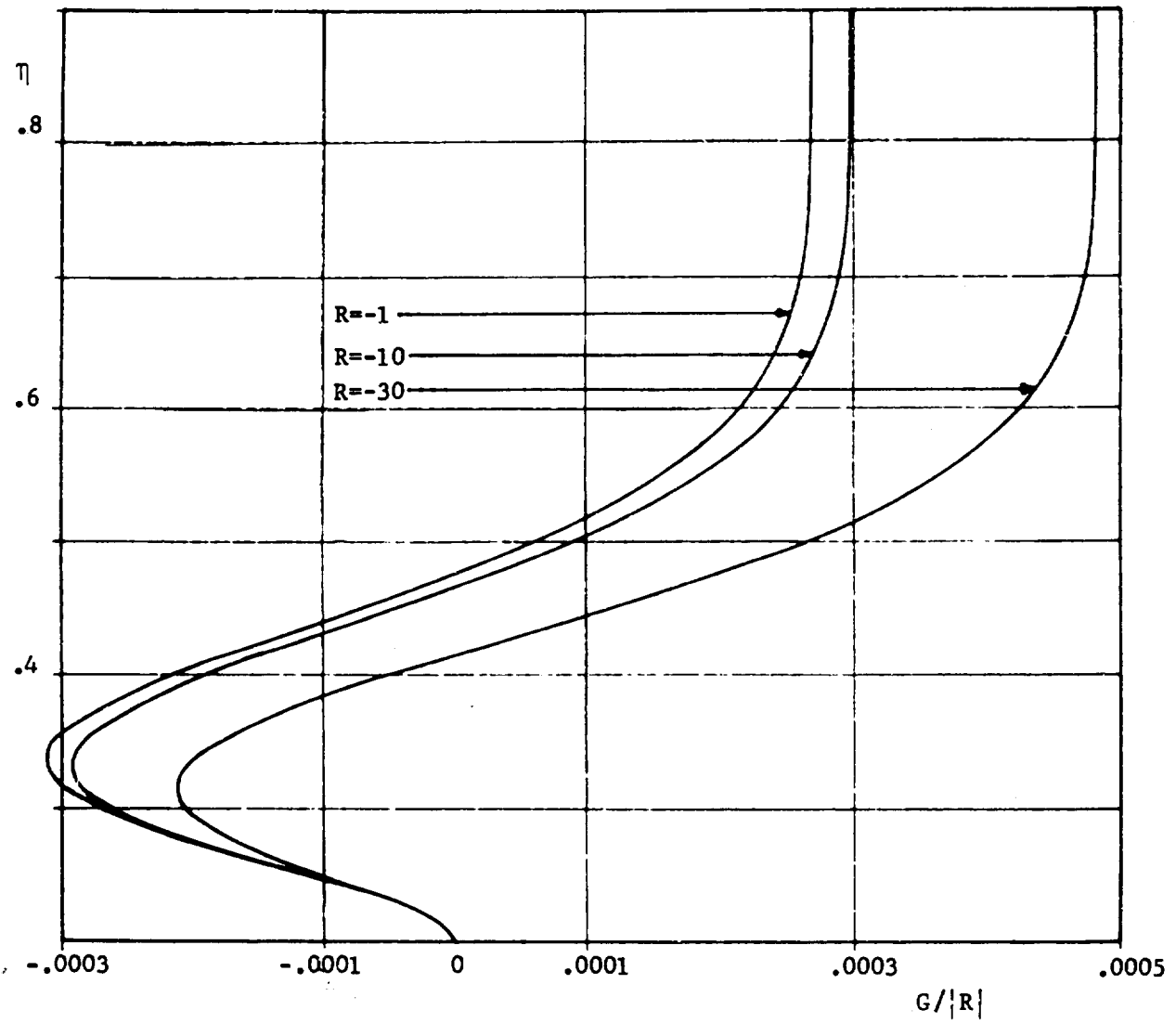

Fig. 12: Axial velocities $G = w_\infty W/2\Omega\ell$ versus dimensionless variable η at velocity ratio $\varkappa = -.22$ and different Reynolds numbers R.

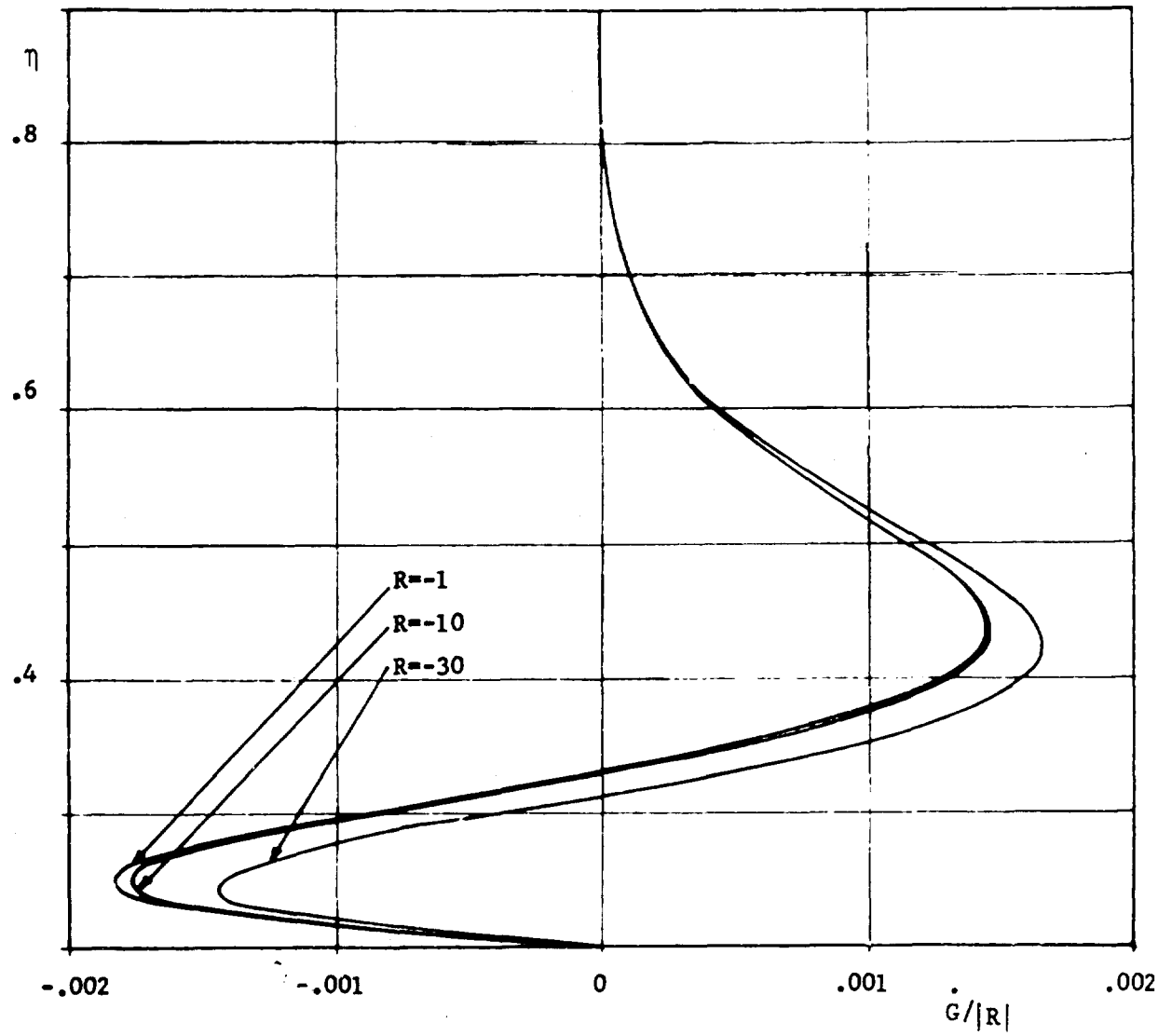

Fig. 13: Radial velocities $\dot{G} = -\dot{U}$ versus dimensionless variable η at velocity ratio $\varkappa = -.22$ and different Reynolds numbers R.

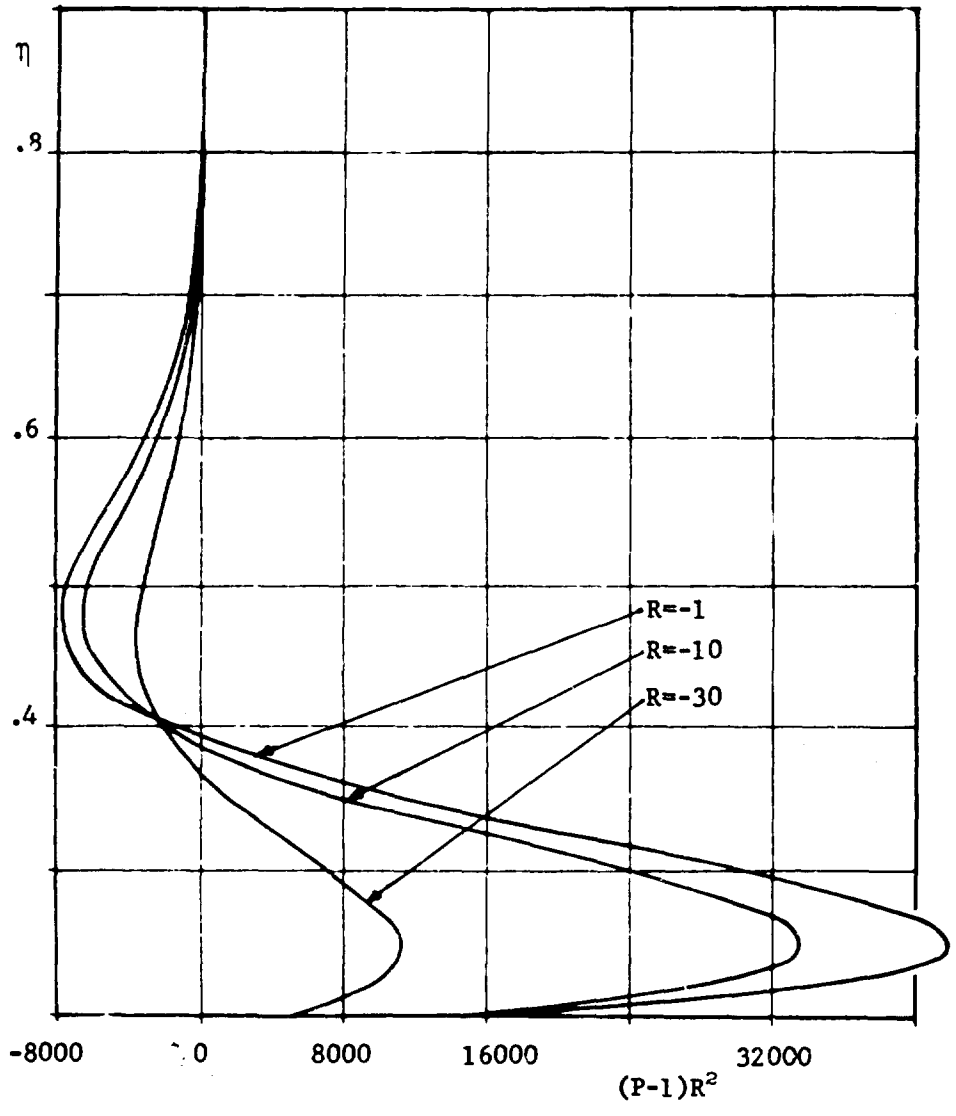

Fig. 14: Pressure functions P versus dimensionless variable η at velocity ratio $\varkappa$ = - .22 and different Reynolds numbers R.